Status Report

MODELING OF CRITICAL LOADS FOR ACID DEPOSITION IN AUSTRIA

Wolfgang Schöpp

SR-91-04
July 1991

MODELING OF CRITICAL LOADS
FOR ACID DEPOSITION
IN AUSTRIA

Wolfgang Schöpp

SR-91-04
July 1991

Preface

Early agreements on international emission reductions have been based on simple source-oriented principles, taking only into account historic levels of national emissions, e.g., the 30% flat rate reduction prescribed in the 'Helsinki Protocol' of the UN/ECE Convention on Long-range Transboundary Air Pollution.

Recent negotiations on further emission reductions introduced effect-oriented approaches as new elements and establish the protection of sensitive ecosystems as the ultimate target of European environmental policy. As a consequence the extent of emission reductions should no longer be determined only by technical and economical considerations, but the requirements to preserve natural ecosystems from damage should become the major principle.

According to current scientific knowledge, in order to quantify the necessary emission reductions threshold levels of exposure below which no environmental damage is expected to occur have to be determined. In this paper the author documents the development of a method to simulate the most relevant acidification processes in forest soils. A comprehensive dynamic formulation of the model system is used to derive static critical loads, which are requested by the negotiation body of the UN/ECE Convention to serve as the basis for the next international protocol.

The application of this approach to Austrian forest ecosystems demonstrates the urgent need to achieve further improvements in air quality in order to protect sensitive forests. The magnitude of the required reductions, together with our knowledge of atmospheric dispersion processes, underlines the absolute necessity not only to focus measures to domestic emission sources, but also to approach emitters outside the Austrian borders.

Markus Amann
Project Leader

Abstract

The author develops an approach to simulate acidification processes in forest soils caused by acid deposition from the atmosphere. Based on a dynamic formulation of the most important processes and external factors leading to soil acificiation the stationary solution of the equation system is derived, which serves as a basis for estimating critical loads for acid deposition. Thereby, critical loads determine the maximum exposure to one or more pollutants, which will not cause chemical changes in the soil leading to long-term harmful effects on the most sensitive ecological systems.

This method is applied to derive critical loads for the Austrian forest soils. Results indicate that acid deposition has to be considered as a potential long-term threat for the majority of Austrian forests. The most sensitive ecosystems occur in the north and north-east of Austria.

A comparison of the critical loads with current acid deposition shows an excess of the threshold limits in large parts of Austria. Certain ecosystems in the east of Austria, in particular forests in the Waldviertel and the oak forests north and south-east of Vienna, face currently an acid deposition of more than ten times above their critical loads.

Finally, a sensitivity analysis identifies the most influential parameters of the model calculations and allows thereby to derive recommendations for further research and monitoring efforts.

Acknowledgments

Contents

Modeling of Critical Loads for Acid Deposition in Austria

Wolfgang Schöpp

1   Introduction

Over the last several decades many areas of Europe have faced increasing acid deposition resulting from growing anthropogenic emissions of acidic substances into the atmosphere [18]. Depending on site-specific conditions, the acid deposition has resulted in severe soil acidification processes in many areas, particularly in forest ecosystems. As a consequence, parts of the observed forest damage can be attributed to increased soil acidification.

In 1985 the UN-ECE Convention on Long-range Transboundary Air Pollution, aiming at an efficient reduction of environmental damage caused by air pollution was signed by 21 countries. Within this convention, negotiations on international reductions of anthropogenic emissions take place on a regular basis. After an initial period of simple 'flat rate reductions' (prescribing equal percentage emission reductions for all signatories) the 'critical loads-concept' became accepted as the major guideline for determining necessary levels of emission reductions. According to this concept, emissions should be reduced until deposition/concentration levels of air pollutants are achieved that "...will not cause chemical changes leading to long-term harmful effects on the most sensitive ecological systems" [1].

Consequently, national and international efforts are currently being undertaken to determine such critical loads for the European ecosystems in order to provide a scientific basis for further emission reduction strategies. This work is internationally harmonized by the 'Coordinating Center for Effects' located at the National Institute for Public Health and Environmental Protection (RIVM) in the Netherlands.

This report describes the results of a study carried out at the request of the Austrian Ministry for Science and Research by the International Institute for Applied Systems Analysis (IIASA). *Section 2* outlines the general approach selected for the determination of critical loads and the basic philosophy of the model. The dynamic formulation of the soil model is developed in *Section 3*. The stationary solution is used to determine the steady-state of the model (*Section 4*), from which critical loads are derived (*Section 5*).

Section 6 gives a short survey on the data acquisition for the Austrian forest soil data base. This data base has been established in cooperation with the Austrian Research Center Seibersdorf (ÖFZS). A sensitivity analysis in *Section 7* identifies the most influential input

1

parameters and derives recommendations for further monitoring work. *Section 8* presents the various critical loads for the Austrian forest ecosystems as a result of the study, and possible directions for further research are discussed in *Section 9*. The report closes with conclusions in *Section 10*.

2   General Approach

Soil acidification is understood to be a dynamic process influenced by a large number of site-specific conditions. In order to put the individual factors influencing soil acidification in relation to each other a systematic framework has been developed. This framework (the 'soil model') enables quantification of the individual processes contributing to acidification.

In contrast to this dynamic understanding, critical loads are defined as the maximum stationary exposure levels to acid input from the atmosphere not causing soil acidification. Consequently, the following approach was selected to derive static critical loads, taking into account the dynamic nature of soil acidification:

- In a first step, a simplified representation of the interaction between the most important factors involved in soil acidification was developed. This 'dynamic soil model' simulates the temporal soil acidification processes as functions of acidic input from the atmosphere, taking into account *inter alia* soil type, precipitation, uptake of nitrogen and base cations by vegetation, and the leaching of nutrients and alkalinity.

- For this dynamic model formulation, a stationary solution was determined that describes a theoretical steady-state with no change in soil acidity if acid input from the atmosphere remains constant.

- This steady-state system is used to determine the maximum acceptable acid input to the particular soil, thereby establishing the critical load.

- The steady-state model also allows a sensitivity analysis to identify the most influential input parameters determining soil acidification.

3   The Dynamic Soil Model

3.1   Modeling approach

To describe the temporal acidification processes of soils, a first attempt has been made to develop a process-oriented model. In order to obtain preliminary results within the time limits set for this study, the model had to be operational with currently available data sets. In a further step,

the model has been used to identify those areas in which additional monitoring would be most beneficial for the improvement of model accuracy.

The model development follows the basic concept described in [11] and comprises the following steps:

- **Identification of the key processes.** Although in reality a variety of different processes influence the soil solution chemistry, the net element input from the atmosphere and the geochemical interaction in the soil (CO_2 equilibrium, weathering of carbonates, silicates and/or Al-hydroxides and cation exchange) have been identified as the key ones. A number of "less important" influences and processes, such as canopy interactions, nutrient cycling processes, nitrogen transformations and organic acid transformations are neglected.

- **Simplified conceptualization of the key processes.** The model describes the interactions of these key processes in simplified form. Interaction of the solute chemistry with the soil compartment is mainly reflected by local parameters (e.g. nitrogen and base cation uptake, silicate weathering) and by equilibrium reactions (e.g. cation exchange). The representation of the solute transport in the model assumes a complete mixing of the element input within one homogeneous soil compartment. If no better information is available a soil layer of 0.5 meter depth is assumed. Furthermore, for simplification, seasonal variations of the water flux are neglected and no long-term change of the hydrology is considered.

Justification for the various assumptions and simplifications in the soil model, as well as a detailed interpretation of the chemical equations can be found in [11].

3.2 Basic formulation of the dynamic soil model

The formulation of the dynamic soil model is based on the anion mobility concept [13] which describes the availability of mobile anions in the soil compartment with the help of stock and flow variables.

The major **stock variables** (z_i) depict

- the quantities of chemical constituents in minerals,

- the storage in the exchange complex, and

- the ion concentration

in the soil solution.

Flow variables (x_j) represent the net input of ions and the leaching of elements.

3

The dynamic nature of the acidification process is reflected by **temporal variables**, e.g. for the concentration of H^+ (g) and of HCO_3^- (x_{10}) ions. These concentrations are determined by equilibrium equations featuring Henry's law (Equation 1) and the charge balance principle (Equation 2).

The description of the model equation system utilizes the variables listed in Table 1.

$$x_{l10} g_l = c_1 \, , \tag{1}$$

$$g_l(t) + z_{l7}(t) + x_{l11} = x_{l9} + x_{l10} \, . \tag{2}$$

The various exchange reactions between the elements stored in the soil (Cation Exchange Capacity (CEC)) are described by Gaines-Thomas equations using concentrations instead of activities. These equations contain selectivity constants for H/BC exchange (k_9) and Al/BC exchange (k_{12}) which define the exchange rates of ions[1]. Since the exchange complex is assumed to comprise only H, Al and BC, the description of the exchange between H/Al is obtained by combining Equations 3 and 4 and assuring that the sum of the fractions adds up to unity.

$$z_{l9}(t)/z_{l6}(t) = k_9 x_{l12}^2(t)/g_l^2(t) \, ; \tag{3}$$

$$z_{l9}^3(t)/z_{l6}^3(t) = k_{12} z_{l8}^2(t)/z_{l7}^2(t) \, ; \tag{4}$$

$$g_l(t) + z_{l8}(t) + z_{l9}(t) = 1 \, . \tag{5}$$

The derivation of the acidity input (x_{l9}) is explained in Section 5.1.

The cation exchange and the dissolution of the buffering minerals depend crucially on the soil type. In the following these processes are described separately for carbonate, aluminum hydroxide and unbuffered systems respectively.

3.3 Carbonate system (Case 1 with $z_{l1}(t-1) > 0$)

In calcareous soils, acidity of the soil water is caused by the formation of bicarbonate from dissolved CO_2, a process that depends on the partial pressure of CO_2 in the soil. Free H^+ produced by this mechanism and by acid input is neutralized by the dissolution of calcite.

In the model, the HCO_3^- concentration x_{l10} is determined as the positive root in the interval [0, 1.0] of the equation:

$$x_{l10}^3(t) + x_{l10}^2(t) x_{l9}(t) - x_{l10}(t) c_1 - c_2 = 0 \, . \tag{6}$$

The H^+ concentration $g_l(t)$ is calculated based on Henry's Law:

$$g_l(t) = c_1/x_{l10}(t) \, . \tag{7}$$

---

[1]In the following the term base cations (BC) is used for Magnesium and Calcium ions.

Table 1: List of variables used in the dynamic soil model

Stock Variables:	
z_{l1}	amount of carbonates
z_{l2}	amount of gibbsite
z_{l3}	SO_2 concentration
z_{l4}	NO_3 concentration
z_{l5}	NH_4^+ concentration
z_{l6}	BC^{2+} concentration
z_{l7}	Al^{3+} concentration
z_{l8}	Al^{3+} fraction in exchange complex
z_{l9}	BC^{2+} fraction in exchange complex
Flow Variables:	
x_{l1}	SO^{2+} deposition
x_{l2}	NO_3^- deposition
x_{l3}	NH_4^+ deposition
x_{l4}	total N deposition
x_{l5}	NO_3^+ input to soil-system
x_{l8}	NH_4^+ input to soil-system
x_{l9}	total acidic load to soil-system
x_{l11}	BC^{2+} amount available per period
x_{l13}	Al^{3+} concentration on input
x_{l14}	BC^{2+} concentration on input
Temporal Variables:	
x_{l10}	HCO_3^- concentration
x_{l12}	H^+ fraction in exchange complex
g_l	H^+ concentration

Table 2: Values of chemical model parameters assumed in this paper

Parameter		Unit	Reference value	Upper	Lower
calcite dissolution	c_2	$(mol\ l^{-1})^3 atm^{-1}$	$10^{-5.83}$	-	-
CO_2 dissolution	c_3	$(mol\ l^{-1})^2 atm^{-1}$	$10^{-7.8}$	-	-
partial pressure of CO_2	c_4	atm	0.02	0.04	0.01
gibbsite dissolution	k_{10}	$(mol\ l^{-1})^{-2}$	$10^{8.77}$	$10^{9.35}$	$10^{8.11}$
nitrification factor	k_3	-	1.0	-	-
ratio of Al to BC weathering	k_{11}	-	2.0	-	-
Gaines-Thomas selectivity constant for Al/BC exchange	k_{12}	$mol\ l^{-1}$	1.0	10.0	0.1
Gaines-Thomas selectivity constant for H/BC exchange	k_9	$(mol\ l^{-1})^{-1}$	$15 * 10^4$	$30 * 10^4$	$7.5 * 10^4$
bulk density	ρ	$g\ cm^{-3}$	1.3	-	-
soil water content	k_1	$m^3 m^{-3}$	0.3	-	-
nitrification factor	k_3	$fraction$	1	1	0

Table 3: Regional model parameters

Parameter		Unit
net input of base cations (=base cation deposition - uptake)	k_5	$mol\,m^{-2}yr^{-1}$
weathering rate	k_2	$mol\,m^{-2}yr^{-1}$
N-uptake by vegetation	k_4	$mol\,m^{-2}yr^{-1}$
1/(annual water flux)	k_{13}	m^{-3}

An equilibrium equation for $CaCO_3$ dissolution is used to obtain the concentration of $Ca^{2+}(BC^{2+})$ ions (z_{l6}):

$$z_{l6}(t) = x_{l9}(t) + x_{l10}(t) - c_1/x_{l10}(t) . \tag{8}$$

Consequently, the amount of carbonates remaining in the soil is calculated by the mass balance:

$$z_{l1}(t) = \max\{0, z_{l1}(t-1) + k_5 - z_{l6}(t)/k_{13} + k_1 z_{l6}(t-1)\} \tag{9}$$

where k_5 represents the net base cation input to the soil, as a result of base cation deposition and base cation uptake of plants.

3.4 The Aluminum system (Case 2 with $z_{l2}(t-1) > 0$ and $z_{l1}(t-1) \leq 0$)

For noncarbonate soils and for soils in which carbonates are exhausted, but where Al-hydroxides or similar minerals are still available, base cation balances and buffering reactions have to be described differently:

In order to derive the availability of mobile cations BC^{2+} in the soil water due to their net input (k_5) and mineral weathering (k_2) a mass balance for base cations is established:

$$x_{l11}(t) = k_5 + k_2 + k_8 z_{l9}(t-1) + k_1 z_{l6}(t-1) , \tag{10}$$

where k_8 is the cation exchange capacity.

The maximum available base cation concentration can be obtained from the base cation amount in solution x_{l11}

$$x_{l14}(t) = k_{13} x_{l11}(t). \tag{11}$$

The following relations can be established for the aluminum system; however, it has to be noted that these equations are only valid if the base cation availability is above a certain minimum concentration (k_6) [19]

$$k_5 + k_2 \geq k_6 > 0. \tag{12}$$

The system of cation exchange and aluminum buffering has to be solved according to equations 1, 2 and 14 – 19. By transforming these equations, the problem is reduced to finding a root in the interval $[0, b_0]$ for x_{l12}. In this analysis the value of the constant b_0 is extracted from Figure 14 in deVries *et al.* [11].

$$\left. \begin{aligned} h_{l1}(t) &= 1 - x_{l12}(t) - k_7 x_{l12}^3(t) ; \\ h_{l2}(t) &= x_{l14}(t) - k_8 k_{13} h_{l1}(t) ; \\ h_{l3}(t) &= k_9 x_{l12}(t)\sqrt{h_{l2}(t)/h_{l1}(t)} ; \end{aligned} \right\} k_{10}h_{l3}^4(t) + h_{l3}^2(t) + h_{l3}(t)(h_{l2}(t) - x_{l9}(t)) - c_1 = 0 , \tag{13}$$

x_{l12} represents the H^+ ions saturated in exchange complex. Using this solution the remaining relations can be determined consecutively.

The various exchange reactions are described by Gaines-Thomas equations using concentrations instead of activities:

- for Al^{3+} ions in the exchange complex:

$$z_{l8}(t) = k_7 x_{l12}^3(t) \tag{14}$$

with:

$$k_7 = k_{10}(k_{11}/k_{12})^{1/2}/k_{12} \; ; \tag{15}$$

- for the BC^{2+} ions in the exchange complex:

$$z_{l9}(t) = 1 - x_{l12}(t) - z_{l8}(t) \; ; \tag{16}$$

- for the BC^{2+} concentration:

$$z_{l6}(t) = x_{l14}(t) - k_8 k_{13} z_{l9}(t) \tag{17}$$

- for the H^+ concentration:

$$g_l(t) = k_9 x_{l12}(t) \sqrt{z_{l6}(t)/z_{l9}(t)} \; ; \tag{18}$$

- for the concentration of Al^{3+} an equilibrium equation for the gibbsite $Al(OH)_3$ dissolution is used:

$$z_{l7}(t) = k_{10} g_l^3(t) \; . \tag{19}$$

The remaining Al-hydroxide in soil is derived from the mass balance equation for aluminum:

$$z_{l2}(t) = \max\{0, z_{l2}(t-1) + k_{11}k_2 - k_{13}^{-1} z_{l7}(t) + k_1 z_{l7}(t-1) - k_8(z_{l8}(t) - z_{l8}(t-1))\}. \tag{20}$$

3.5 Non-carbonate soil without Al-hydroxide (Case 3 with $z_{l2}(t-1) \leq 0$)

For non-carbonate soils in which Al-hydroxide is exhausted the equation describing solubility does not apply and has therefore to be removed from the system. Since the solubility of Fe is not included in this model, the description is only valid above a certain pH-value.

As in the previous case, the BC^{2+} input is calculated by the mass balance:

$$x_{l14}(t) = k_{13}(k_5 + k_2 + k_8 z_{l9}(t-1) + k_1 z_{l6}(t-1)) \tag{21}$$

To solve this equation an initial value of the Al^{3+} input must be determined. For reasons of simplicity, a first estimate assumes the weathering of a base cations proportional to the

8

aluminum weathering. Consequently, also in this case a factor k_{11} can be used to describe the weathering, enabling the formulation parallel to Equation 21:

$$x_{l13}(t) = k_{13}(k_{11}k_2 + k_8 z_{l8}(t-1)) .$$

(22)

The system of cation exchange must be solved as described in Equations 1, 2, 17, 24, 16, 18, 24, 19. A transformation of these equations reduces the problem to Equation 23.

Exchangeable BC^{2+}, z_{l9} can be determined by finding a root in the interval $[0, x_{l12}(t) / k_8 k_{13}]$:

$$
\left.
\begin{aligned}
h_{l4}(t) &= x_{l14}(t) - k_8 k_{13} z_{l9}(t) ; \\
h_{l5}(t) &= h_{l4}(t)/z_{l9}(t) ; \\
h_{l6}(t) &= \sqrt{h_{l5}(t)} ; \\
h_{l7}(t) &= x_{l13}(t)/(k_{12}h_{l6}(t)h_{l5}(t) + k_8 k_{13}) ; \\
h_{l8}(t) &= x_{l13}(t) - k_8 k_{13} h_{l7}(t) ; \\
h_{l9}(t) &= 1 - z_{l9}(t) - h_{l7}(t) ; \\
h_{l10}(t) &= k_9 h_{l9}(t) h_{l6}(t) ;
\end{aligned}
\right\}
\quad h_{l10}(t)(h_{l10}(t) + h_{l8}(t) + h_{l4}(t) - x_{l9}(t)) - c_1 = 0 .
$$

(23)

For the other ions, the system can be solved in the following sequence:

- For BC^{2+} concentration there is no difference to the case with aluminum buffering. Equation (17) holds:

$$z_{l6}(t) = x_{l14}(t) - k_8 k_{13} z_{l9}(t) ;$$

- Al^{3+} ions in an exchange complex can be determined by substitution of the equation (25) in the Gaines-Thomas reaction equilibrium (4):

$$z_{l8}(t) = x_{l13}(t)/(k_{12}\sqrt{z_{l6}^3(t)z_{l9}^{-3}(t)} + k_8 k_{13}) ;$$

(24)

- Thereby, the Al^{3+} concentration is

$$z_{l7}(t) = x_{l13}(t) - k_8 k_{13} z_{l8}(t) ;$$

(25)

- and the H^+ ions in the exchange complex:

$$x_{l12}(t) = 1 - z_{l8}(t) - z_{l9}(t) .$$

(26)

- The H^+ concentration determines to

$$g_l(t) = k_9 x_{l12}(t)\sqrt{z_{l6}(t)/z_{l9}(t)} .$$

(27)

9

4 The Steady-State Soil Model

For given conditions (soil types, acid inputs etc.), the dynamic soil model outlined above can be used to determine the steady-state of acidification, i.e., the stage at which no further acidification processes occur. Within this study such steady-state solutions are used to derive the maximum net input of acidity not causing acidification of soils, thus defining the 'critical load'.

Such steady-state solutions of the dynamic model can be interpreted as the stationary solution given a constant input of acidity to the soil. The time needed to reach such a final state is not significant in this approach.

The actual determination of the stationary solution of the dynamic model depends on the existence of calcite and gibbsite.

4.1 Carbonate systems

There is always a slight dissolution of calcite which does not effect the stationary status, because in most carbonate systems the availability of calcite is almost infinite. Therefore, depletion would only occur after exceedingly long time periods. Steady-state solutions in carbonate systems show constant values over time for all other variables. If, however, only a limited amount of calcite is available, the analysis has to follow the procedure described for aluminum systems.

4.2 Aluminum systems

In aluminum systems, a solution is defined as stationary if no dissolution of gibbsite (Al-hydroxide) occurs and all other variables stay constant (Equation 30). At such a status a buffering or neutralizing capacity still exists.

By definition, in aluminum systems the amount of ions in the soil is constant. Consequently, there is no exchange between the cation exchange complex and the soil solution and concentrations depend only on the net input of ions. Based on Equations 10, 17, 1, 20 and 2 the equation system can be reduced for base cations (BC^{2+}) to:

$$z_{l6} = (k_5 + k_2)k_{13}/(1. - k_1 k_{13}) \,, \tag{28}$$

$$g_l + k_{10}g_l^3 + z_{l6} = x_{l9} + c_1/g_l \,, \tag{29}$$

and for Aluminum (Al^{3+}) to: [2]

$$k_{10}g_e^3 < k_{11}k_2k_{13}/(1. - k_1k_{13}) .$$

(30)

4.3 Noncarbonate soil without Al-hydroxide

This case is very similar to the above system except that aluminum concentration is determined by the input of aluminum ions, as is the BC-concentration. Therefore, the solution of the system can be performed as outlined above.

$$z_{l7} = k_{11}k_2k_{13}/(1. - k_1k_{13}) ,$$

(31)

$$g_l + z_{l7} + z_{l6} = x_9 + c_1/g_l .$$

(32)

Soils in this class are very acidic. For any steady-state solution in this range it has always to be assured that (a) the resulting level of acidity is within the range over which the model is defined and (b) no transition to another soil class has occurred, taking into account acidification processes at natural levels of acid deposition.

---

[2]For the given range of parameters, there is just one positive real solution of this 4th order polynom. The analytical formula can be found as follows:

$$p(y) = d + xy + y^2 + ay^4$$

$$p = \frac{-1}{9a^2} - \frac{4d}{3a}$$

$$q = \frac{1}{27a^3} + \frac{2d}{3a^2} - \frac{4d - x^2}{2a^2}$$

$$r = p^3 + q^2$$

$$s = \frac{1}{3a} - \frac{p}{(q + \sqrt{r})^{\frac{1}{3}}} + (q + \sqrt{r})^{\frac{1}{3}}$$

$$\frac{\frac{-x}{2a\sqrt{-\frac{d}{a} + \frac{s^2}{4}}} + \sqrt{\frac{x^2}{4a^2\left(-\frac{d}{a} + \frac{s^2}{4}\right)} - 4\left(\frac{s}{2} - \sqrt{-\frac{d}{a} + \frac{s^2}{4}}\right)}}{2}$$

5 The Derivation of Critical Loads

As discussed above, at a constant acid deposition rate there exists a level of soil acidification at which no further acidification occurs – the so called 'steady-state'. Consequently, steady-state solutions can also be used to determine the maximum net input of acidity that does not lead to critical levels in the soil chemistry.

For forest soils, the exact limits are difficult to define. However, for the Aluminum system, research results indicate that Al-concentrations occurring at pH levels of soil solution around 4.5 – 4.2 may have negative impacts on the growth of fine roots [15]. Such pH ranges in forest soils imply a concentration of Al^{3+} below 2 mg/l. According to Equations 1 and 20 the corresponding critical alkalinity amounts to ($alk = -z_{e7} - g_e + x_{e10}$) of -300.10^{-6} eq/l.

The Ca:Al and BC:Al ratios in the soil can be introduced as additional criteria. Results from the ALBIOS research project [4] and Johnson [14] conclude that for sensitive tree species (in particular Red Spruce, followed by Sugar Maples, Douglas Fir and Beach) plant growth is reduced at Ca:Al ratios of less than 0.7 – 2.0. Scots Pine, Oak and Birch seem to be less sensitive.

The corresponding critical loads for net acid input x_{l9} can be determined according to the following system:

$$x_{l9} \leq z_{l6} - alk \ . \tag{33}$$

For a BC:Al ratio of one:

$$x_{l9} \leq 2z_{l6} + (z_{l6}/k_{10})^{1/3} - c_1(k_{10}/z_{l6})^{1/3} \ . \tag{34}$$

5.1 The calculation of net acid input

Estimates of atmospheric deposition at a given location can be used to determine the net input of cations NH_4^+ and strong acid anions SO_4^{2-} and NO_3^-.

In order to derive the amount of ions available for soil chemistry reactions it is assumed that all SO_4^{2-} penetrates into the soil, and that some of the NH_4^+ and NO_3^- is partly taken up by the vegetation and partly transformed from reduced nitrogen compounds to nitrates (nitrification). Consequently, a part of the deposited ammonia ($x_{l3}(t)$) changes to oxidized nitrogen and thus adds to the NO_3^- intake.

The total available nitrogen (x_{l4}) sums up to:

$$x_{l4}(t) = x_{l2}(t) + x_{l3}(t) + k_1(z_{l4}(t-1) + z_{l5}(t-1)) \ , \tag{35}$$

The NO_3^- input into the system (x_{l6}) is computed by subtracting a fraction of the N-uptake by vegetation with k_4 as the potential N-uptake of the plants. Thereby, the total input of oxidized nitrogen is determined by

$$x_{l6}(t) = x_{l5}(t) - k_4(x_{l5}(t) + k_1 z_{l4}(t-1))/x_{l4}(t) , \qquad (36)$$

with the nitrification factor $0 \leq k_3 \leq 1$:

$$x_{l5}(t) = x_{l2}(t) + k_3 x_{l3}(t) . \qquad (37)$$

The parameter k_1 denotes a field capacity, z_{l3}, z_{l4} and z_{l5} the equivalent concentrations of SO_4^{2-}, NO_3^-, and NH_4^+ ions in soil water.

In all cases the regional data set must be checked for consistency in order to assure that the N-uptake is lower than the available nitrogen.

Parallel calculations are made for NH_4^+:

$$x_{l7}(t) = (1 - k_3)x_{l3}(t) , \qquad (38)$$

$$NH_x: \quad x_{l8}(t) = x_{l7}(t) - k_4(x_{l7}(t) + k_1 z_{l5}(t-1))/x_{l4}(t) , \qquad (39)$$

The solute transport of elements is described by assuming a complete mixing of all input elements. The concentration of available mobile ions ($SO_2^{2-}, NO_3^-, NH_4^+$) in soil water at one time step can therefore be computed by the mass balance equations:

$$[SO]_4^{2-}: \quad z_{l3}(t) = k_{13}(k_1 z_{l3}(t-1) + x_{l1}(t)) , \qquad (40)$$

$$[NO]_3^-: \quad z_{l4}(t) = k_{13}(k_1 z_{l4}(t-1) + x_{l6}(t)) , \qquad (41)$$

$$[NH]_4^+: \quad z_{l5}(t) = k_{13}(k_1 z_{l5}(t-1) + x_{l8}(t)) , \qquad (42)$$

with k_{13}^{-1} as the total amount of water passing a soil compartment during the year (field capacity + percolation). The initial conditions for these equations are:

$$(z_{l1}(0), \ldots, z_{l6}(0)) = (z_{l1}^{init}, \ldots, z_{l6}^{init}) . \qquad (43)$$

The described formulation of the dynamic soil model requires only the acidic load as input. Therefore, a new variable x_{l9} is introduced to represent the sum of charges available for chemical reactions in the soil. This is the linking variable between the acid input and the model:

$$x_{l9}(t) = z_{l3}(t) + z_{l4}(t) - z_{l5} , \qquad (44)$$

The input of Al^{3+} and BC^{2+} depends on the state of the soil and has been discussed in an earlier section.

6 Data Acquisition

For this study, data collection was mainly performed by the ÖFZS and the Institut für Analytische Chemie of the Technical University Vienna. More detailed descriptions on the applied methodologies can be found in the relevant documentations.

6.1 General data

The model approach described above requires a number of regional parameters to determine the critical load for a given ecosystem. The following data bases have been used to derive relevant data:

- The inventory of soil types in Austria based on unpublished work by Prof. Fink [16].

- Geological hydrological data extracted from the "Hydro-Geologische Karte für Österreich aus dem Österreich-Atlas" [16]

- Information on land-use in Austria (forest/no forest area) combined with forest-type data.

- Soil types according to FAO classification derived by overlaying the above mentioned maps.

- Precipitation patterns estimated on information developed by the Technical University Vienna.

- Evapotranspiration data from Baumgartner et al. [17] have been corrected for deciduous (+240 mm/yr) and coniferous (+120 mm/yr) forests; for northward-oriented slopes ($\pm 67.5°$) with an inclination larger than 30%, a 30% lower evapotranspiration rate has been assumed. The corrections were adapted with a constant value so that the total water balance for Austria did not change.

6.2 Ion depositions

Due to the specific orography, major local variations in acid deposition occurs throughout Austria. Therefore, data on acid deposition had to be derived on a small spatial scale inventory on precipitation for all of Austria, available at the Institut für Analytische Chemie at the Technical University Vienna [7].

However, within the ongoing international negotiations on agreements for further emission reductions, maps of critical loads will be used for comparison with deposition patterns computed by atmospheric long-range transport models with a spatial resolution of 150x150 km grid (the EMEP model) [2].

In order to derive the local deposition from the average grid deposition computed with the EMEP model the following approach has been developed:

Wet depositions: The measured sulfur and nitrogen concentrations in rain water were spatially interpolated and superimposed with a map of local precipitation.

Dry depositions: The measured concentrations of air pollutants in rural areas have been spatially interpolated. Based on this regional distribution, dry deposition has been calculated with the help of a deposition velocity factor.

The resulting maps of total acid deposition and sulfur deposition (including the forest filtering) are displayed in Figures 1 and 2.

Within this project the described method has been tested and compared with the measured deposition at some EMEP measuring stations in Europe. Results are contained in Annex I.

6.3 Soil characteristics

The necessary model input data describing the soil characteristics can be derived from the available soil map. Relevant data on soil characteristics were compiled at an international expert meeting held at IIASA in Spring 1990 (Table 4 and 5). Values displayed in these tables have been adopted by the Coordination Center for Effects as a general guideline for the international mapping exercise [6].

As soon as further information from ongoing monitoring studies in Austria becomes available, these data can be verified and – if necessary – replaced by more accurate information. Preliminary data used in this study are listed in Table 4.

The parameter values for the various weathering classes in Table 5 have been extracted from [6] and the report of a Workshop on 'Critical Loads for Nitrogen and Sulphur' held in Skokloster, Sweden in 1986 [1].

6.4 Biomass uptake

In this study the biomass uptake of base cations and nitrogen has been estimated based on the canopy type by relating the annual biomass increment [3] to the proper element contents [5]. Data are available for trees in areas with moderate and low concentrations of elements in soil. At very high or very low concentrations of base cations or nitrogen in soil water, additional processes are becoming important that may lead to systematic errors. In order to provide consistency for low concentrations, the computed potential uptake has to be checked against the availability of nutrients in the soil. Data on forest growth and element contents are displayed in Table 6.
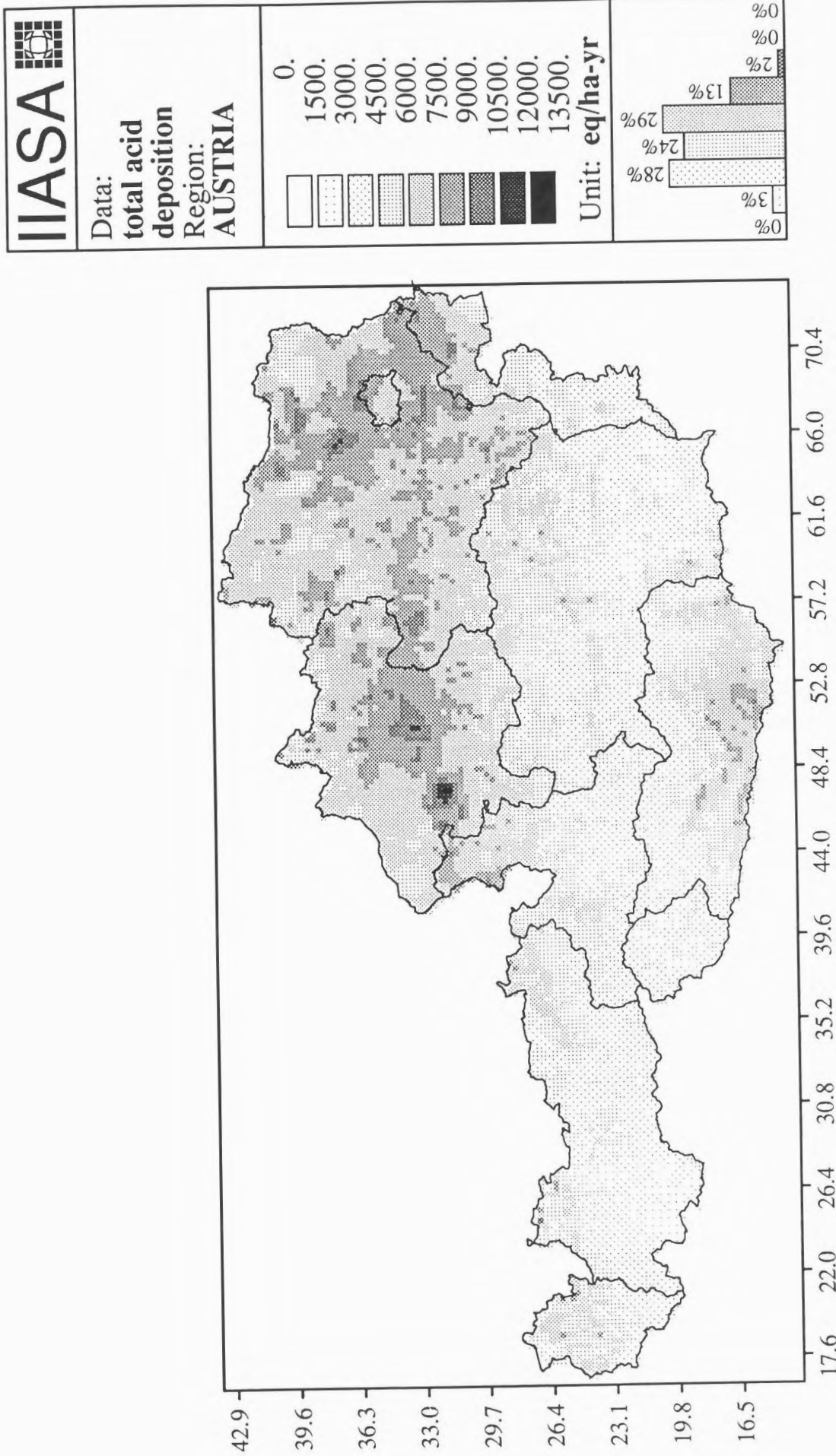
15

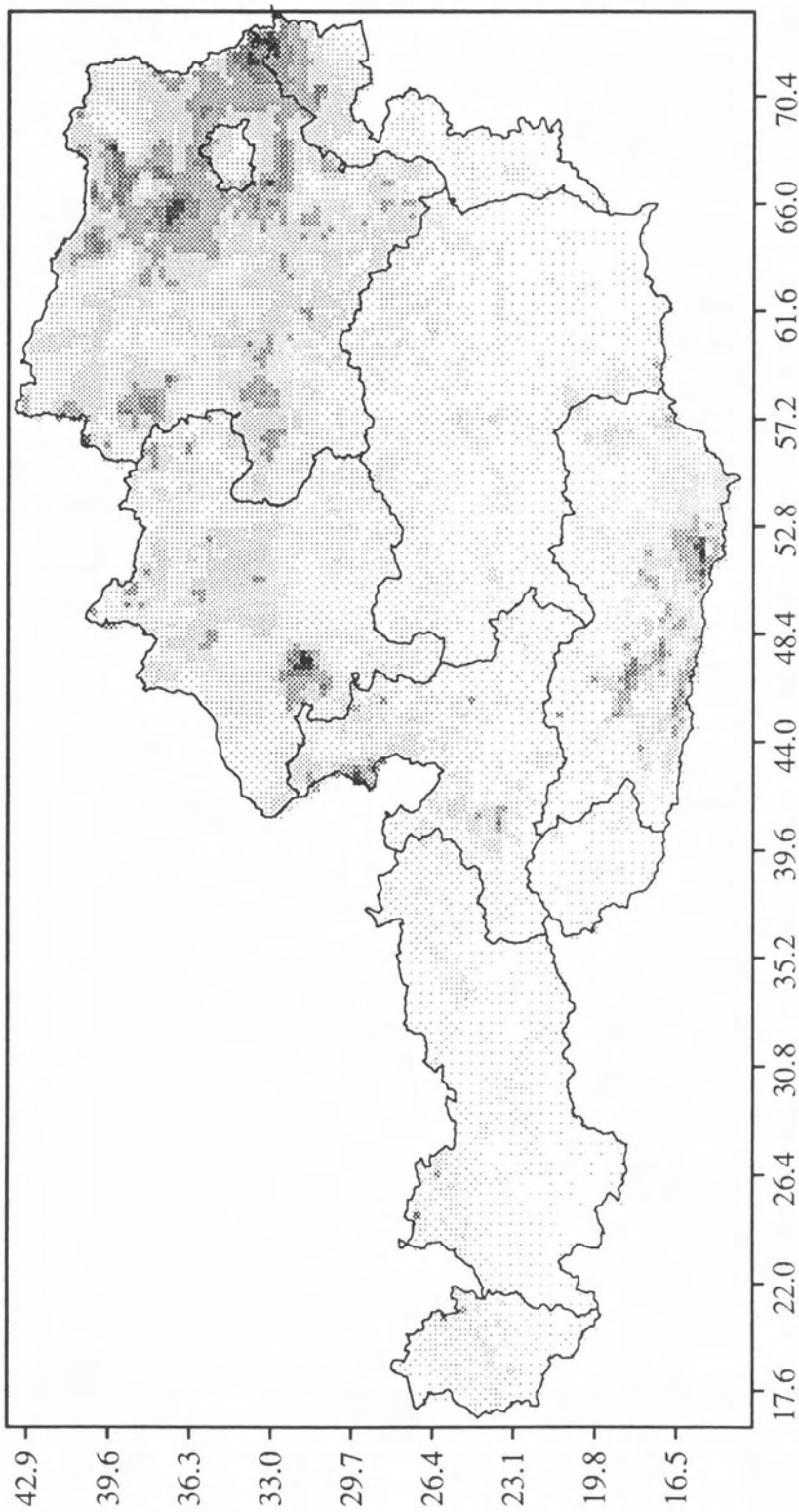Figure 1: Total acid deposition (including the forest filtering) in 1985 (Source: Kovar [7])
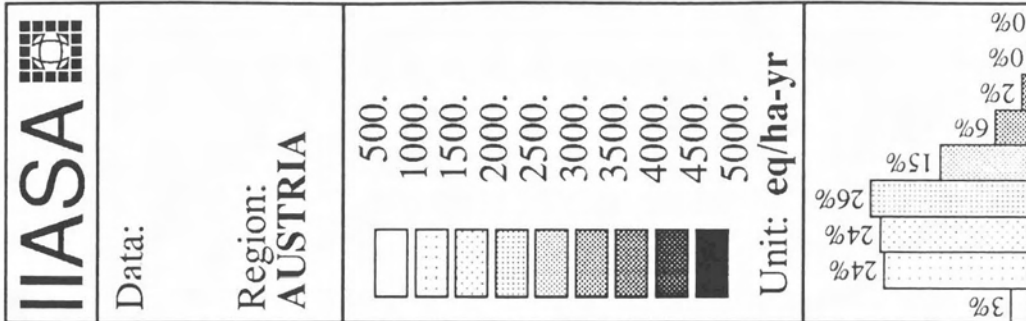
Figure 2: Sulphur deposition (including the forest filtering) in 1985 (Source: Kovar [7])

IIASA

Data:

Region:
AUSTRIA

500.
1000.
1500.
2000.
2500.
3000.
3500.
4000.
4500.
5000.

Unit: **eq/ha-yr**

Table 4: Data for soil characteristics

Soil type			clay %	cec eq/m^3	CaCO$_3$ %	bas. sat.	field cap.	weather. class
Lithosol a. Kalk	Eutric Lithosol	Ie	5.	350.	90.	1.	0.36	10*
Lithosol sonst.	Dystric Lithosols	Id	5.	182.	0.	.15	0.04	2
Ranker	Rankers	U	13.	360.	0.	.30	0.20	3
Regosols	Calcaric Regosols	Rc	22.	155.	0.	.45	0.22	3
Rendsina (alpin)	Orthic Rendzinas	Eo	29.	520.	20.	1.	0.40	6*
Rendsina (sonst.)	Rendzinas	E	0.	650.	0.	.30	0.20	2
Parabraunerde	Orthic Luvisols	Lo	27.	300.	0.	.6	0.45	4
Schwarzerde	Chernosem	Ch	40.	520.	5.	.9	0.4	4
Braunerde a.K.	Eutric Cambisols	Bec	23.	380.	5.	8.	0.4	10
Braunerde sonst.	Dystric Cambisols	Bd1	16.	221.	0.	.4	0.27	1
Braunlehm, Rotlehm	Eutric Cambisols	Be1	49.	456.	0.	.8	0.3	4
Reliktboden a.K.	Eutric Cambisols	Be2	23.	380.	.5	.1	0.4	5
Reliktboden sonst.	Dystric Cambisols	Bd2	30.	300.	0.	.3	0.21	3
Podsol	Orthic Podsol	Po	2.	156.	0.	.1	0.15	1
Podsol A-Horiz.	-	-	-	350.	-	-	-	-
Pseudogley+Rel. Pg.	Gleyic Luvisols	Lg	30.	300.	0.	.25	0.4	5
Semipodsol	leptic Podsols	Pl	13.	91.	0.	.150	.17	1
Paratschnernosem	Luvic Phaeozems	Hl	18.	300.	0.	.7	0.10	3
Feuchtschwarzerde	Haplic Phaeozems	Hh	18.	429.	1.	.15	0.4	2
Hochmoore	Dystric Histosols	Od	0.	500.	0.	.15	0.7	0
Niedermoore	Eutric Histosols	Oe	15.	500.	5.	.19	0.6	0
Auböden, Graue	Eutric Fluvisols	Je	10.	252.	20.	1.	0.2	10
Auböden, Braune	Dystric Fluvisols	Jd	20.	200.	1.	.5	0.3	3
Gleye a.Kalk	Eutric Gleysols	Ge	25.	300.	5.	1.	0.3	10
Gleye sonst.	Dystric Gleysols	Gd	30.	400.	0.	.4	0.4	5

* At altitudes above 1500 m set to 1.

Source: Based on [6].

Table 5: Weathering rates ($mol_c ha^{-1} yr^{-1} m^{-1}$) in various classes.

Weathering class	Weathering rate	Values used in this study
1	0 - 500	500
2	500 - 1000	1000
3	1000 - 1500	1500
4	1500 - 2000	2000
5	2000 - 2500	2500
6	2500 - 3000	3000

Table 6: Data on element contents (in %)

| Tree species	Stem (kg/m^3) density	Stem Content %				Branch Content %				Ratio Branch/ Stem	Forest increment (m^3/ha/yr)
		N	Ca	Mg	K	N	Ca	Mg	K		
Scotch pine	490	0.11	0.09	0.02	0.05	0.40	0.24	0.05	0.20	0.15	5.0
Douglas fir	410	0.08	0.05	0.01	0.05	0.31	0.50	0.06	0.26	0.10	8.9
Norway spruce	450	0.10	0.12	0.02	0.06	0.57	0.34	0.07	0.37	0.15	10.
Oak	740	0.19	0.20	0.05	0.13	0.37	0.50	0.05	0.19	0.38	7.0
Beech	860	0.13	0.09	0.03	0.09	0.44	0.27	0.03	0.16	0.23	7.0
Coniferous	500	0.10	0.08	0.02	0.05	0.35	0.35	0.05	0.25	0.15	10.
Deciduous	700	0.15	0.10	0.04	0.10	0.45	0.50	0.05	0.20	0.2	7.0
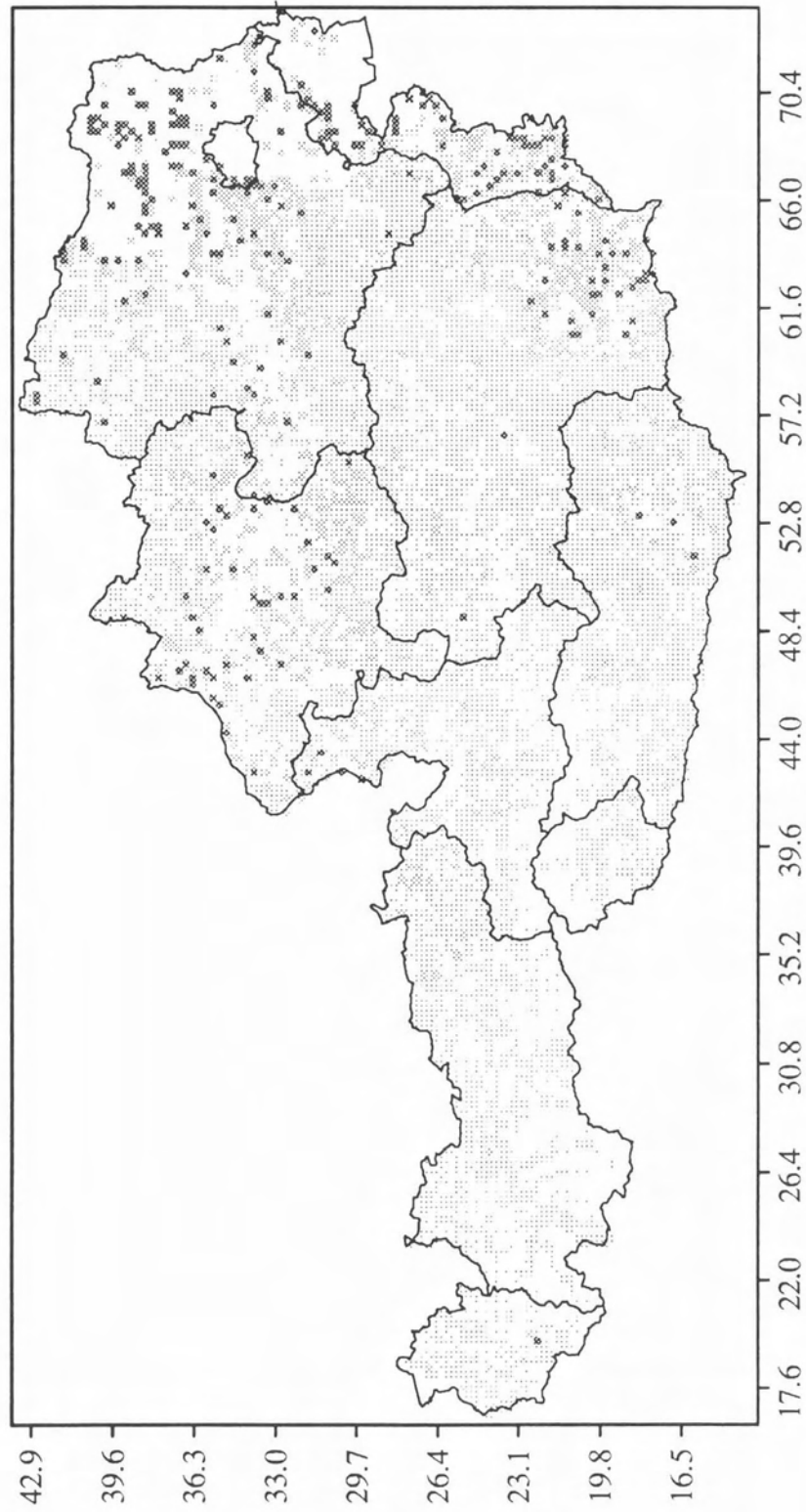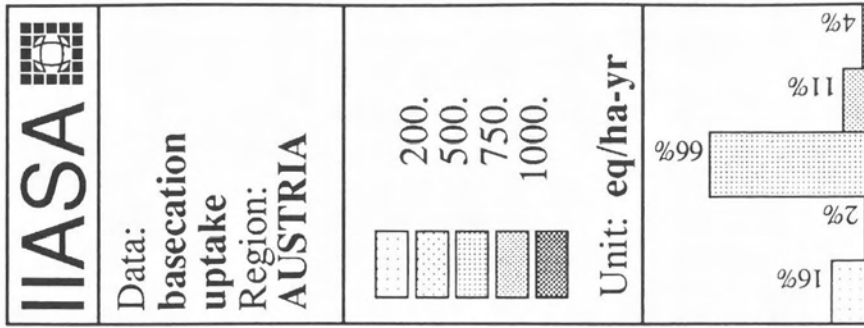
Figure 3: Uptake of base cations by forest ecosystems in Austria

6.4.1 Base cation uptake by forestry management

Plants take up more cations than anions for their nutrients balance from the soil. To balance out this cation deficit in the nutrients exchange, the vegetation releases protons to the dissolution of the soil. In natural forests the cations stored in the biological mass of the plants will be returned to the soil during decomposition. However, if harvested trees are removed from the forest ecosystem (e.g. by forest management) the incorporated base cations are also extracted from the system. Similar imbalances can also occur in natural forests, when the organic substance decomposes extremely slowly (e.g. in the formation of thick litter-layers in the subalpine forest region). The uptake of base cations by forest ecosystems in Austria is shown in Figure 3.

In this analysis it has been assumed that all forests are managed in Austria, i.e. that wood is retrieved from the forest after harvesting. No provisions, however, are made for systems with slow decomposition.

7 Sensitivity analysis

The reliability of model results depends strongly on data quality. As listed above, the approach developed in this study requires a large amount of input data, which are not always easy to monitor. Therefore, and in order to focus data acquisition efforts on the most influential local parameters, the relevance of the various input data was recognized with the help of a sensitivity analysis.

7.1 Potential impacts of model variables

In a first step the analysis identified the potential interrelationships of the individual model parameters and qualitative impacts of parameter changes on model results.

Results of this analysis are presented in Table 7. The diagonal in this table represents the direct impacts of variables on soil acidification; indirect impacts via other variables are displayed in the non-diagonal fields.

The following example should help to interpret this table: Variation of the parameter values for surface runoff is taken here as an example. If the surface runoff increases, nutrients from the litter layer are washed out. However, this effect is to a certain extent compensated by less anions entering other soil layers. Therefore, the overall impacts on soil acidification are negligible (marked as '0'). At the same time less water percolates through the soil leading to a higher concentration of ions in the soil water (indicated by '+').

Table 7: The direct and indirect effects of physical/chemical variables on soil acidification. Positive impacts are indicated by +, negative by −.

Variable	Effects through							
	Percolation	Forest growth	BC uptake	N uptake	Weath. rate	N dep.	Sulfur dep.	BC dep.
Surface runoff	+	0	0	0	0	0	0	0
Precipitation	−	0	0	0	0	+	+	−
Percolation	−	0	0	0	0	0	0	0
Forest growth	0	(+)	+	−	0	0	0	0
Base cations uptake	0	0	+	0	0	0	0	0
Nitrogen uptake	0	0	0	+	0	0	0	0
Weathering rate	0	(+)	0	0	−	0	0	0
Nitrogen dep.	0	(+)	0	(−)	0	+	0	0
Sulfur deposition	0	0	0	0	0	0	+	0
Base cations dep.	0	(+)	(+)	0	0	0	0	−

7.2 Uncertainty in model parameters

This chapter will discuss the effects of model parameters on soil acidification and critical loads computed with the steady-state model. Since high Al concentration and the Al/Ca ratio are the important factors for vegetation damage the analysis is restricted to the Al-buffer range only.

7.2.1 Uncertainties of chemical parameters

In the steady-state version of the soil model the gibbsite dissolution k_{10} is the only chemical parameter having influence in the Al-buffer range. Figure 4 displays the variation of soil pH for three particular values for this parameter in dependency of the balance of base cation concentration and total acid load.

As shown in Figure 4 the pH value is very sensitive to changes of the gibbsite dissolution in that range, where base cation concentration is lower than the total acid load. If base cation concentration exceeds the acid load, variation of the gibbsite dissolution does not influence soil acidity. This effect has to be kept in mind when comparing model results with measured pH values.

Figure 5 displays the variation of Al concentration as a function of the difference of base cation concentration and total acid load. Although the response behavior of the Al concentration is similar to that of the soil pH in Figure 4, the absolute variations are considerably smaller for
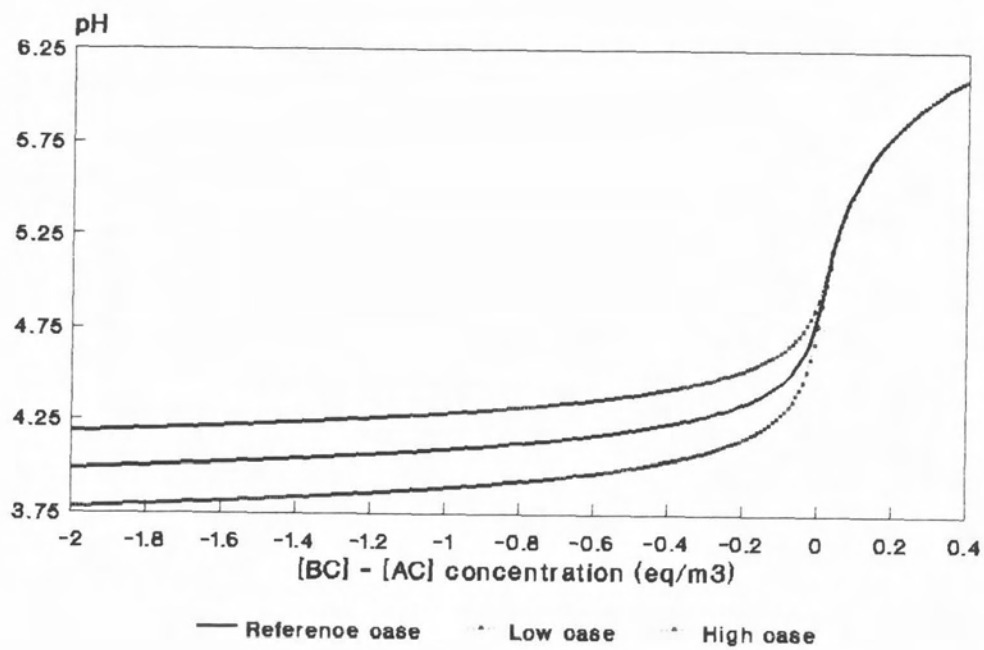
Figure 4: pH of soil as a function of (base cation concentration – total acid load)
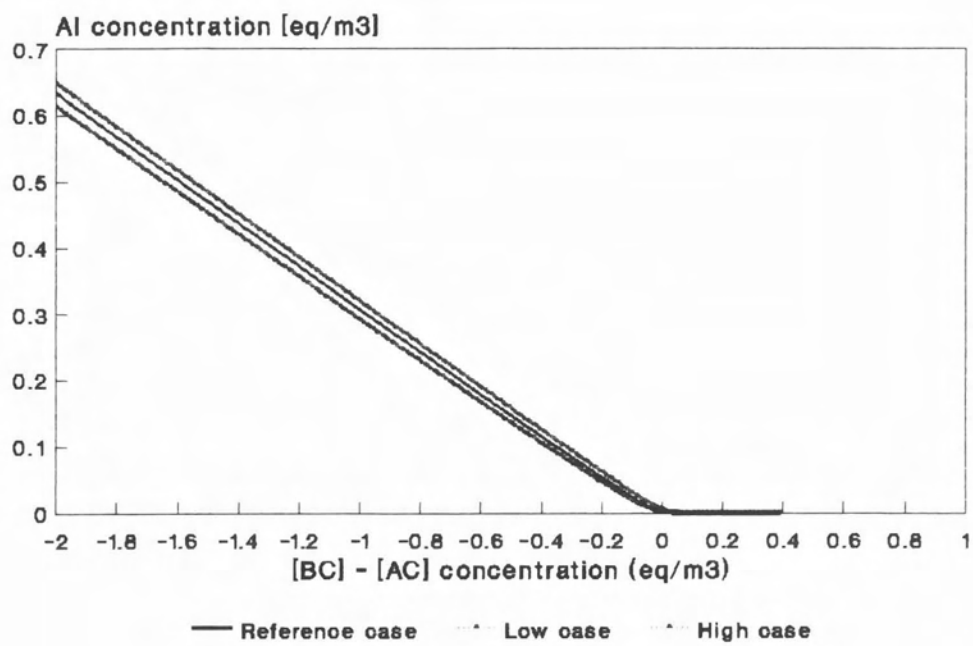
Figure 5: Al concentration in soil solution as a function of the balance (base cation concentration – total acid load)

Al concentration. Consequently, if the gibbsite dissolution is unknown it seems advisable for monitoring programs to primarily analyze Al concentrations instead of soil pH.

7.2.2 Uncertainties of the regional parameters

In the model formulation described above, base cation input and percolation are considered as regional parameters, both associated with considerable uncertainties.

Whereas the Al concentration in the Al-buffer range is linear with the deficiency of the base cation concentration in soil (Figure 5), the resulting changes in soil pH is highly nonlinear (Figure 4). The highest relative sensitivity occurs at the beginning of the buffer range, where base cation concentration and acid loads are in the same range.

This means that the model is rather sensitive only in the aluminum range where acid load is higher than the base cation input. Whereas acid load usually can be determined with some certainty, estimates of deposition, uptake and weathering are associated with large unknowns. Thereby, reliable model results crucially depend on the quality of the base cation data.

To explore the regional impacts of modified base cation data on the model results for Austria, Section 8 analyzes a case where the default base cation deposition as recommended by the UN-ECE has been substantially increased, taking into account the specific Austrian situation. In contrast for example, to the Nordic countries, forest area in Austria is typically mixed with agricultural area, representing (together with road dust) an important source of the base cation input to forests. Analyze carried out by Ivens [18] found that at comparable sites in Europe total base cation deposition (including dry deposition) is typically twice that of the wet deposition rate. In Map 7 of Section 8 this has been taken into account by increasing the base cation input by 400 eq/ha/yr, which is about the minimum wet base cation deposition in Austria.

Further, an additional correction has been introduced for areas with low percolation. In this study percolation is calculated as the difference between precipitation and evapotranspiration. Consequently, the relative uncertainty of computed percolation data is largest when this difference approaches zero. To reduce the potential errors introduced by this method, a general rule applied by civil engineering has been incorporated by fixing the minimum percolation in dry areas to 5% of the local precipitation value (Section 8, Map 8).

8 Model results

This chapter presents the results of the application of the steady-state version of the soil model on the Austrian forest ecosystems. Maps are presented for critical loads and for steady-state pH.

8.1 General findings

The study shows that a considerable part of forest soils in Austria are in areas where soil acidification may occur. Vegetation is most sensitive on soils in the silicate or cation exchange buffering range. At these locations soils do not naturally acidify, but high H^+ concentration can emerge due to acid depositions from the atmosphere.

However, in some areas of the subalpine, the alpine and the northern regions of Austria with low decomposition rates, acidification might be considered to a certain extent as a natural process (Map 1). Since, over centuries of selection, the ecological systems here have adapted to the acid environment, forests in these areas are to some extent resistant to acidity [9]. However, if the buffering capacity is depleted, an additional acid load will cause acidification of ground and surface water. Increased leaching of nutrients caused by continued acid deposition might also cause a deficit in nutrients availability to the forests, in particular a shortage of Mg ions [19].

8.2 Interpretation of the maps

Grid shaded maps create the impression that the displayed value would be applicable to the entire shaded area. This is misleading for two reasons: First, often not all the area within the grid is actually covered by forests; and second, the grid data reflect the representative situation within the grid. Subgrid variations are possible, but ignored in this study. The values presented in the map refer neither to particular points nor to specific areas, but reflect the most typical results for the grids. Consequently, some further validation of the maps has to be done if specific ecosystems are to be analyzed on a smaller scale.

One should therefore not focus on single grid values. The reader is asked to form regional clusters with similar characteristics and to draw conclusions only for such regions.

In the following, three types of maps are presented:

- Maps displaying the steady-state pH values;

- Maps of critical loads for forest soils; and

- A map displaying the excess of acid deposition over critical loads.

8.3 The steady-state pH of forest soils in Austria

The steady-state pH has been calculated for two sets of input data.

Since the steady-state has not been evaluated for carbonate soils, such areas are excluded from calculations. However, to consider such carbonate soils in the alpine regions, which are

sensitive to acidification, all soils above 1500 meter have been treated as Podsols. Thereby, the 'Kalkalpen' can be included into the map.

Due to the restriction of the applied method only pH values in the range between 6.2 (silicate buffering) and 3.1 (aluminum buffering) are calculated accurately. Model results outside this range just indicate the actual buffer regime of the soil.

MAP 1: The steady-state soil pH for the background case

A 'background case' simulates the 'natural' acidification processes if all acid input of anthropogenic origin is neglected. This theoretic case assumes the adjusted minimum percolation, low base cation input (Section 7.2.2), and an acid load 80% lower than the 1985 values reflecting some assumed level of acid deposition from only natural sources.

According to the map the "Waldviertel", "Mühlviertel", "Bucklige Welt", "Rosaliengebirge" and "Hochschwab" are areas where natural acidification processes are probable (taking a pH of 4.2 as a threshold value).

In order to derive indications of the distribution of undisturbed acidity regimes, the pH-values of this map can be compared with the buffer ranges introduced by B. Ulrich:

- The carbonate buffer range (pH > 6.2),

- the silicate buffer range (pH 6.2 - 5.0),

- the cation exchange buffer range (pH 5.0 - 4.0),

- the aluminum buffer range (pH 4.0 - 3.1), and
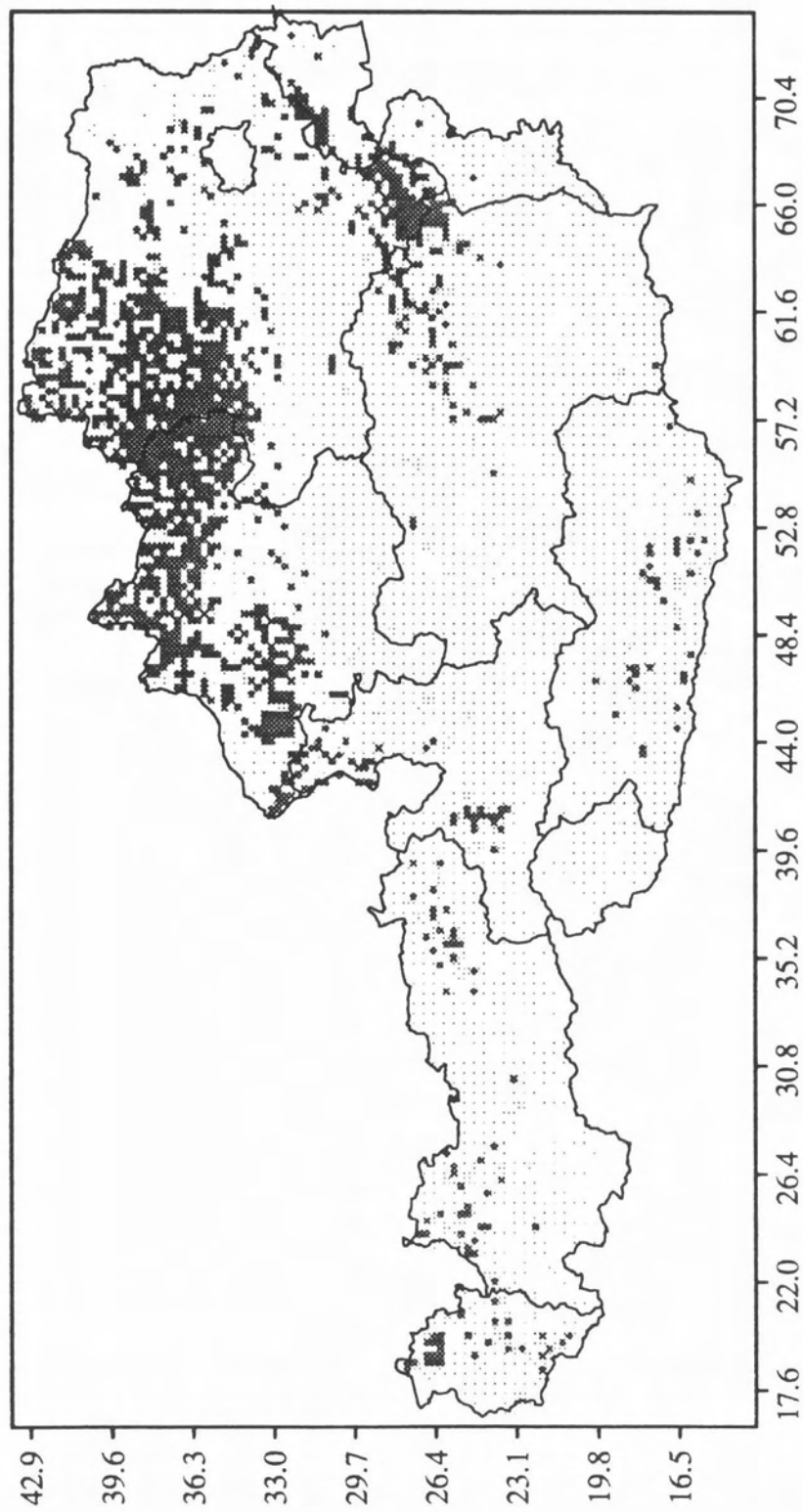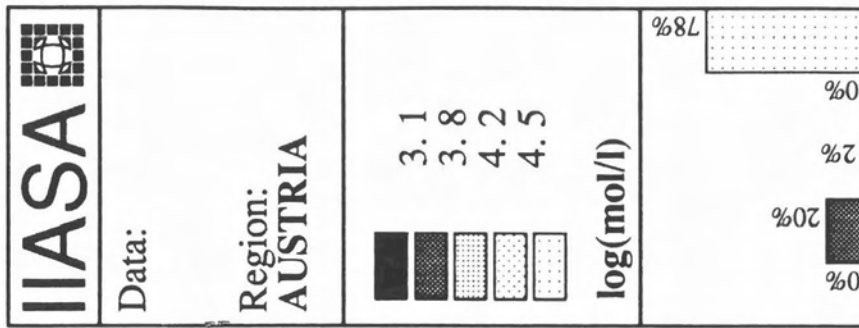
- the iron buffer range (pH < 3.1).

Figure 6: Map 1: pH values of forest soils for the background case

Data:

Region:
AUSTRIA

3. 1
3. 8
4. 2
4. 5

log(mol/l)

20%   2%   0%   78%
0%

29

MAP 2: The steady-state soil pH for the base case

The second case (the 'base case') explores the realistic situation assuming adusted minimum percolation, increased base cation input, and the observed 1985 deposition of acid compounds as constant load.

Results show that the anthropogenic input drops the pH value in most ecosystems at least by one class (i.e. buffer range according to Ulrich) below the background case of Map 1. At some locations, irreversible processes are to be expected that will completely change the characteristics of soils by washing out all clay minerals. Thereby, these soils will loose their filtering mechanism and storing capacity of nutrients. This effect has to be expected in the black shaded areas in the alpine region.

In the "Mühl- and Waldviertel", where precipitation is considerably lower, high Al concentration with a loss of nutrients availability occurs and areas move to the Fe-buffer range with pH lower than 3.1.

These results indicate that acidification has to be considered at least as a potential long-term problem for most forests in Austria.
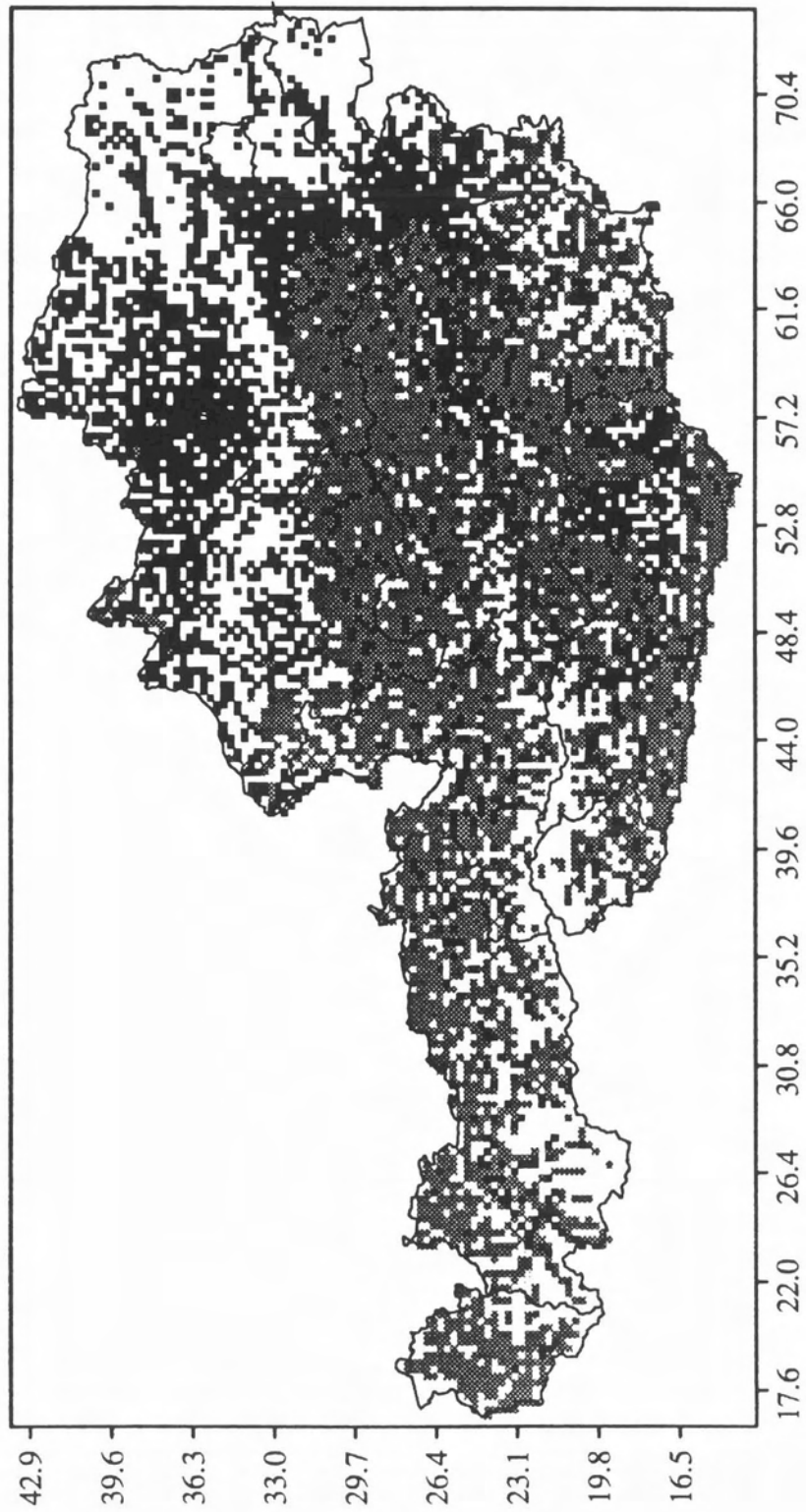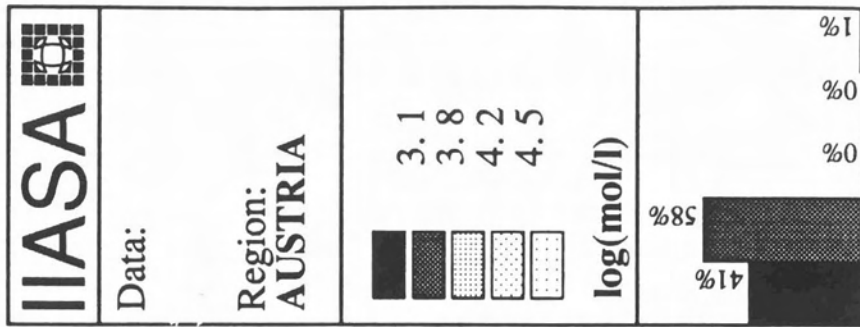
Figure 7: Map 2: Steady-state pH values of forest soils for the base case

MAP 3: Critical loads of actual acidity

Maps 3 to 5 display different formulations of critical loads as defined and required by the UN-ECE. Consequently, they make use of parameter values recommended by UN-ECE. It has to be mentioned that in many cases these recommended values reflect conservative assumptions, leading to relatively low estimates of critical loads. In Map 7 some of these assumptions are modified.

According to the UN-ECE definition critical loads for actual acidity have to take into account base cation weathering processes and assume a maximum leaching of acidity from the soil. They thereby reflect the level of acid input at which the Al concentration in the soil does not exceed $0.2 \, eq/m^3$, which is assumed as a safe level for vegetation. At the same time, acidification caused by forest growth and the neutralization through base cation input are ignored. Thus, existing uncertainties on these factors are excluded and this formulation of critical loads can be used for international comparisons.

As shown in Map 3 critical loads of actual acidity are lowest in dry areas, where Podsoils or Dystric Campisoils occur. This applies in the Wald- and Mühlviertel and on south facing alpine granite slopes. High precipitation in the Alps and in the Kalkalpenvorland result in high critical loads. However, one should keep in mind that special effects which may occur in carbonate soils are not reflected by this model.

On request of the UN-ECE this map has been submitted as the official Austrian contribution to the international mapping exercise coordinated by the Coordination Center for Effects in the Netherlands.
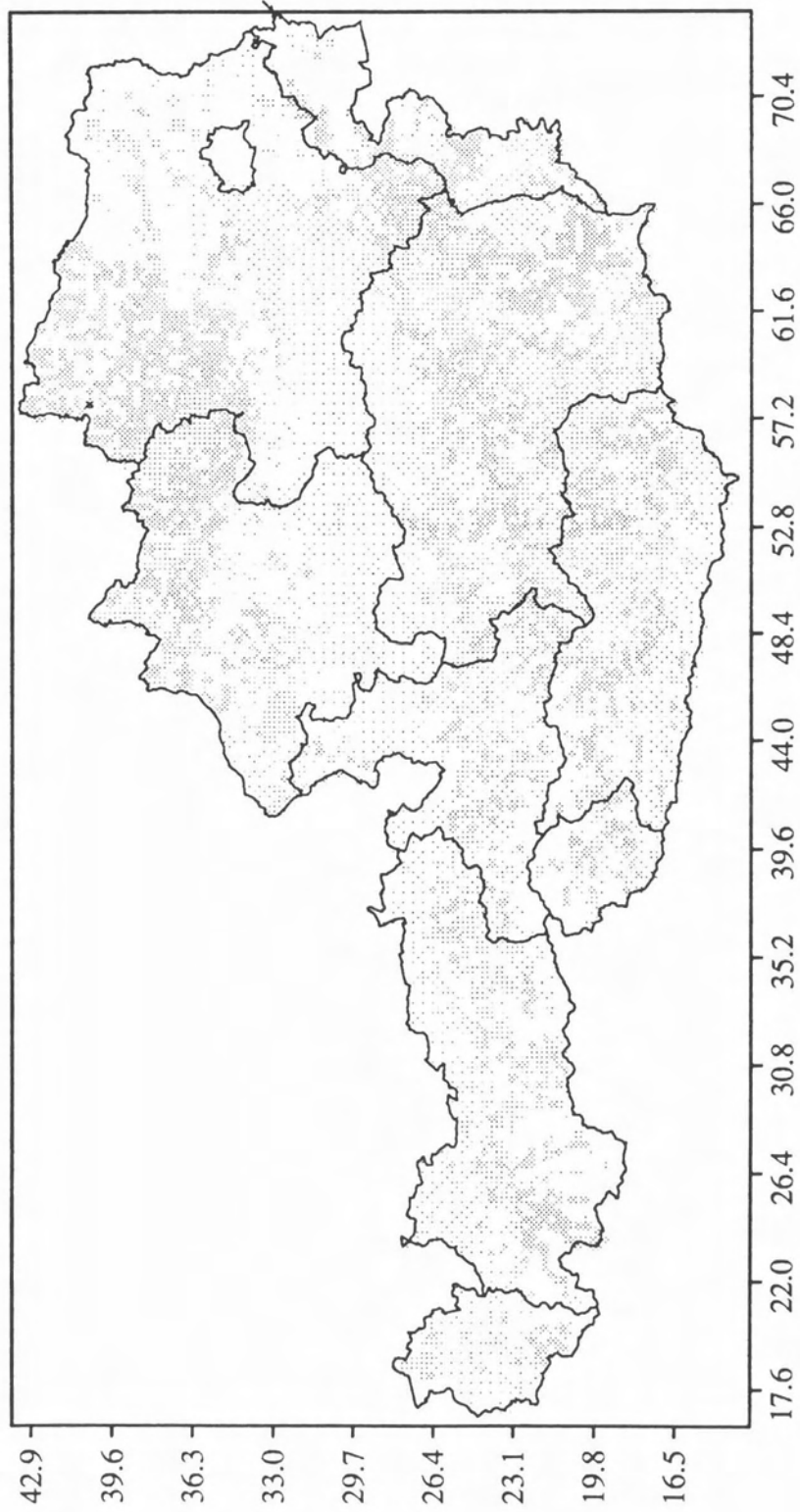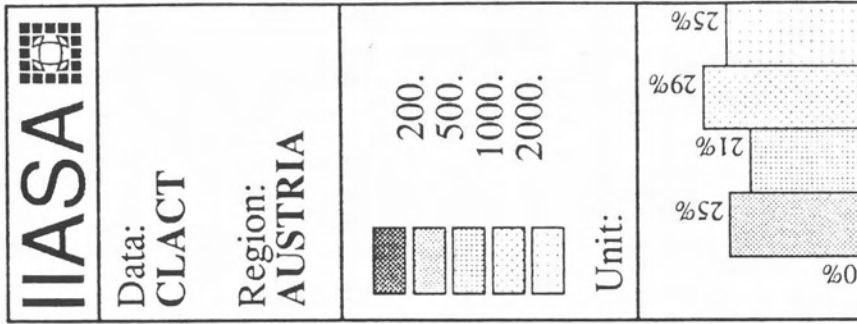
Figure 8: Map 3: Critical loads for actual acidity

MAP 4: Sulfur fraction of actual critical load

Following the philosophy elaborated by the UN-ECE bodies, the critical loads for actual acidity should be split into sulfur and nitrogen fractions to simplify the use of these data for the design of international abatement strategies under the Convention on Long-range Transboundary Air Pollution. It has to be stated that such a breakdown is basically arbitrary and can not be based on scientific logic. Taking this into account, the relevant bodies of the UN-ECE Convention have decided to apply the ratio of sulfur and nitrogen deposition in 1985 to the actual critical loads and thereby derive the desired fractions.

Such a split is not only arbitrary, but may also lead to incorrect conclusions. Since critical loads for nitrogen are derived from the values for actual acidity, they do not incorporate the potential limitations of nitrogen deposition necessary to avoid eutrophication. In some cases, however, eutrophication could require more strict critical loads for nitrogen than result from the officially adopted procedure. Critical loads for sulfur, as obtained by this procedure may be lower than necessary than if the correct critical loads for nitrogen (referring to eutrophication) had been established.
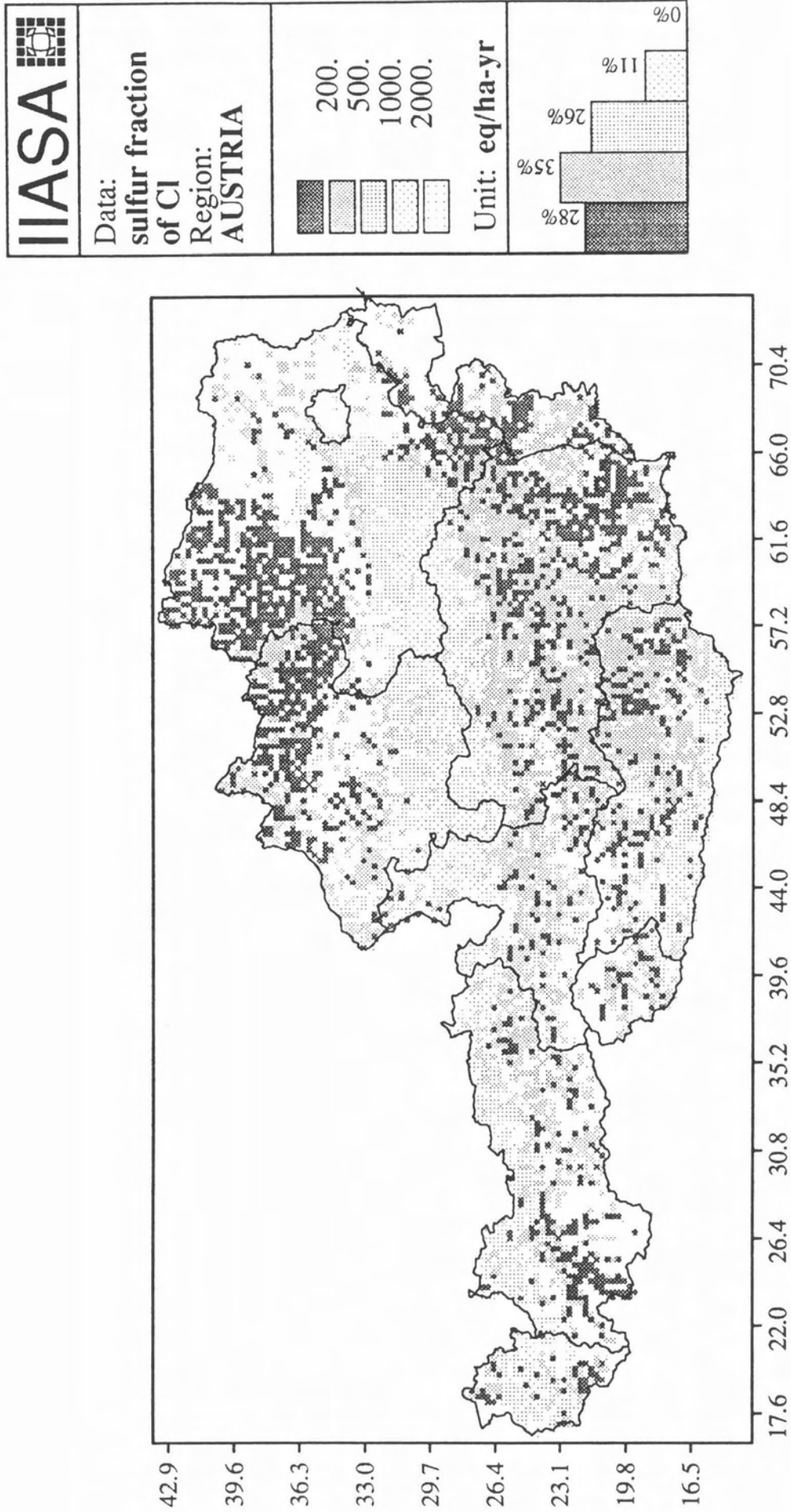
Figure 9: Map 4: Sulfur fraction of actual critical loads

MAP 5: Critical loads for sulfur deposition

In order to compare the maps of actual critical loads displayed with the deposition of air pollutants, the following additional factors have to be considered:

- Base cation uptake by vegetation,

- uptake of nitrogen by vegetation, and

- deposition of base cation from the atmosphere.

As a conservative assumption this study only considers the long-range contribution of wet base cation deposition, and ignores dry deposition as well as base cations originating from local sources. However, it has to be stated that the poor quality of the currently available data on base cations introduces a factor of considerable uncertainty into the calculation. Additional research activities to clarify these questions are crucial to improving the reliability of the conclusions.

In Map 5, the actual critical loads for sulfur (Map 4) have been corrected by the factors listed above (applying the sulfur fraction also to the base cation deposition and uptake).

Lowest critical loads for sulfur deposition occur basically in those areas where the critical loads for actual acidity (Map 3) are already low (Wald- und Mühlviertel and dry areas in the alpine region). Consideration of the 'sulfur fraction' increases the sensitivity in the northern part of the country, whereas it is partly compensated for by the base cation deposition in the south.
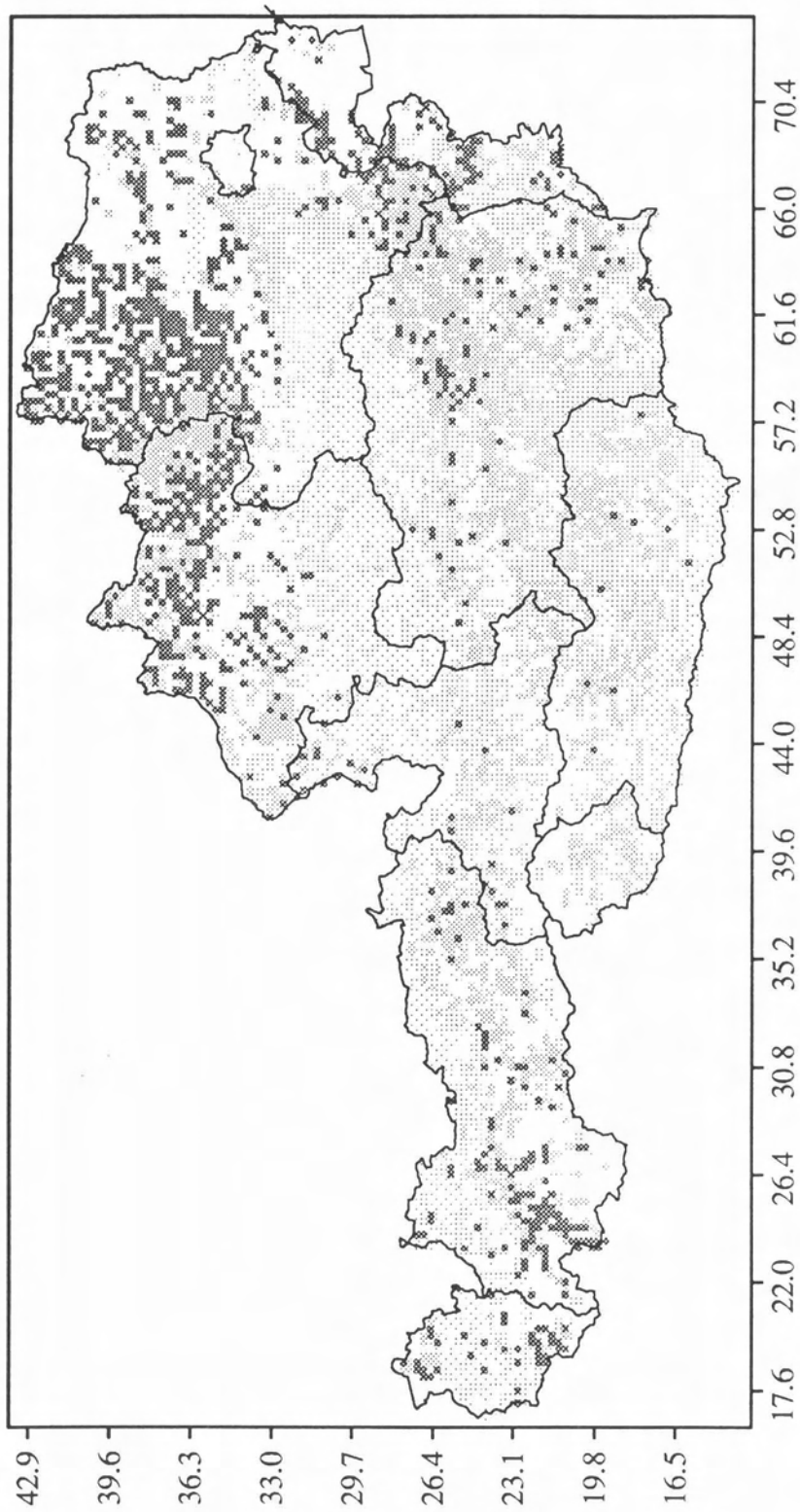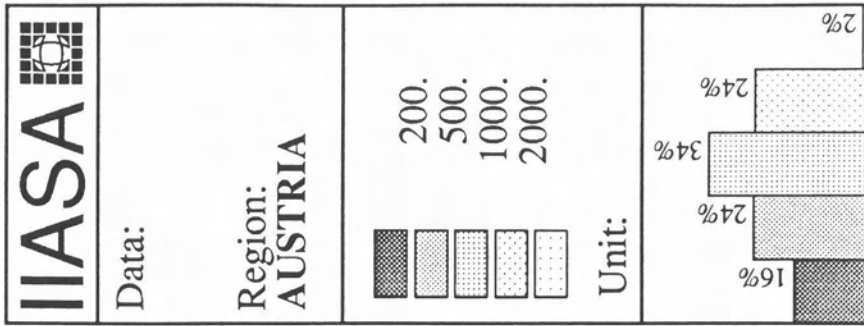
36

Figure 10: Map 5: Critical loads for sulfur deposition

MAP 6: Exceedance of critical loads

This map compares total acid deposition (from SO_2, NO_x and ammonia emissions) from the year 1985 with the critical loads for total acidity as presented in Map 3, corrected by base cation input and nitrogen uptake. The scale of the map expresses total acid deposition as a ratio of the critical loads, i.e. a ratio of 1 means that total acid deposition equals the critical load. Numbers larger than 1 mark the areas where critical loads were exceeded in 1985.

Due to inherent model uncertainties (in particular caused by the limited spatial resolution of the underlying maps) no firm conclusions should be drawn for areas where the model calculates exceedances of up to a factor of two. However, large areas show significantly higher exceedance values which are definitely larger than model uncertainties. This applies in particular to areas of the Wald- and Mühlviertel, where deposition is typically more than five times above critical loads.

The highest exceedances, however, are computed for the oak forest in the 'Weinviertel' north of Vienna. Several reasons contribute to this situation:

- Low dilution caused by low precipitation results in high Al concentration in the soils.

- The dry deposition of sulfur is high due to the relative vicinity of this area to sulfur emission sources (probably outside of Austria).

- Oak forests have high uptake of base cations from the soil.

The high exceedances of critical loads in the area south-east of Vienna (in the 'Leitha Gebirge' and the 'Wechsel') are caused by the specific geologic situation, relatively low precipitation, and by high acid deposition resulting both from Austrian sources as well as from sources located north-east of this area in Hungary and Czechoslovakia.
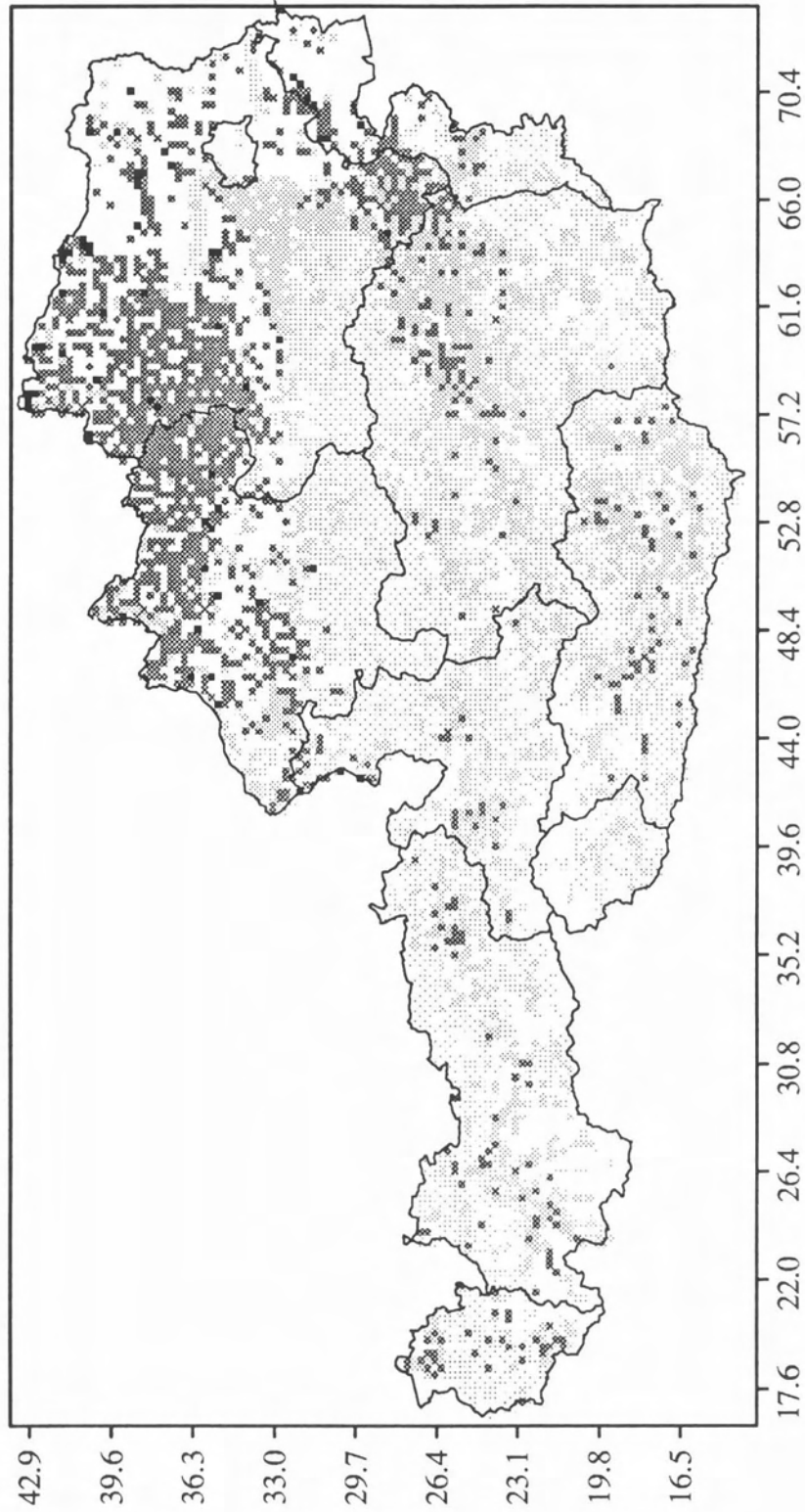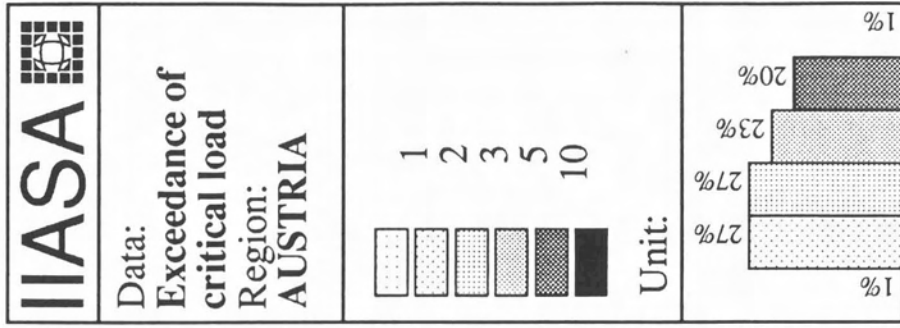
Figure 11: Map 6: Exceedance of the critical loads in 1985

MAP 7: Critical loads for sulfur deposition with increased base cation input

As pointed out in Section 7, present data on base cation deposition are associated with large uncertainties; unfortunately this has substantial impacts on the calculation of critical loads. In order to explore the possible variations of model results, base cation deposition has been generally increased by 400 eq/ha/yr, reflecting higher dry deposition in Central Europe (see also Section 7.3).

The effects of this modified assumption on the critical loads for sulfur deposition are displayed in Map 7. Due to the increased base cation input the two most sensitive classes of critical loads do not occur any more in Austria (compare Map 5), whereas only a few changes occur in other classes. Uncertainty in base cation deposition has therefore a strong relative impact to sensitive ecosystems with low critical loads.
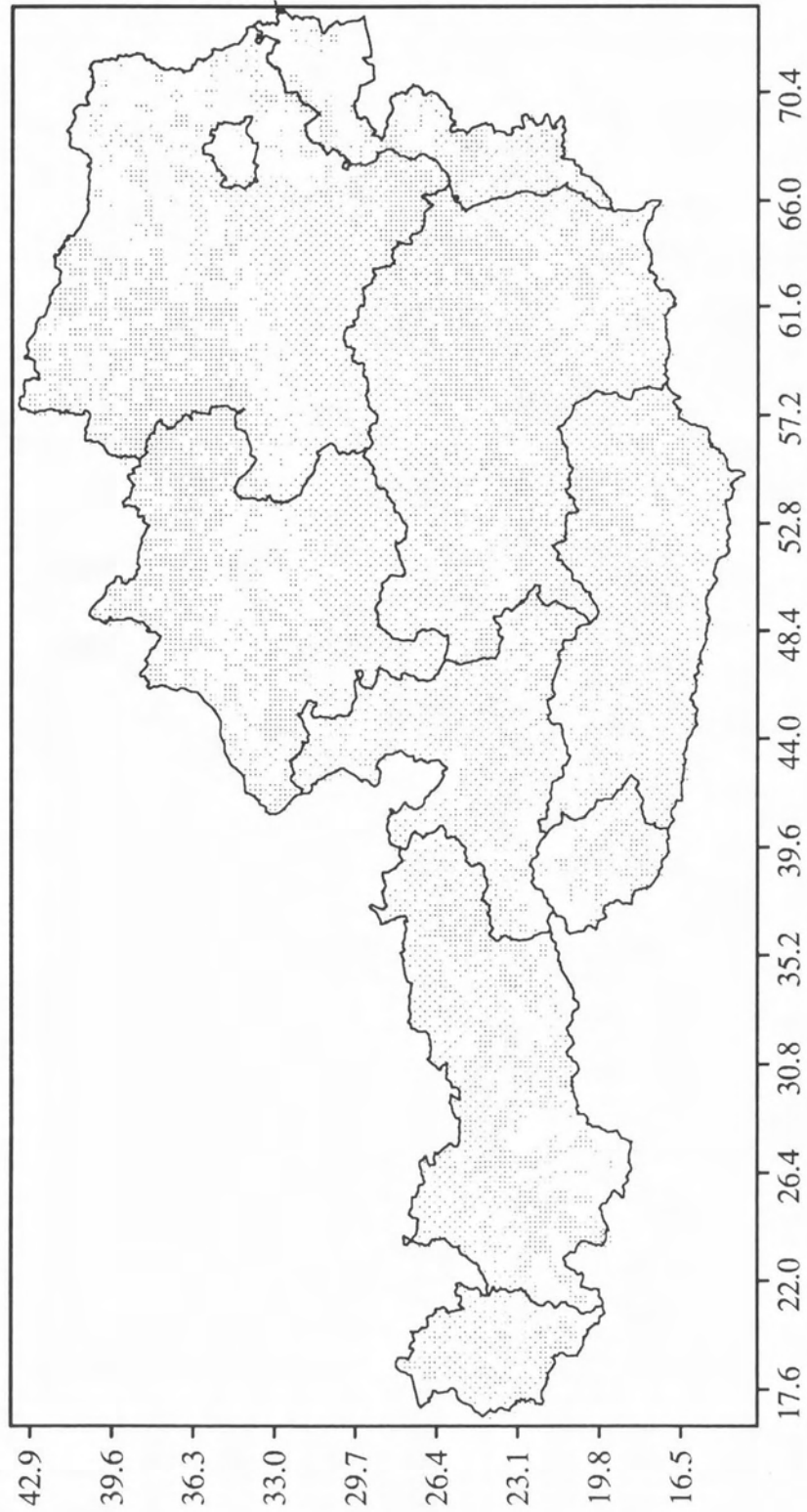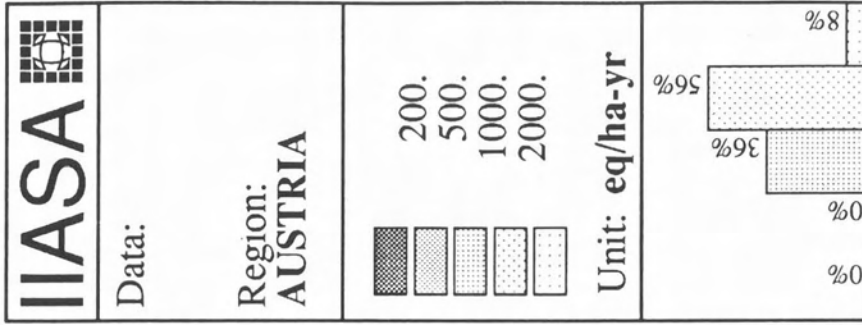
Figure 12: Map 7: Critical loads for sulfur deposition with increased base cation input

IIASA

Data:

Region:
AUSTRIA

200.
500.
1000.
2000.

Unit: **eq/ha-yr**

41

9   Further work

This study has to be considered as a first attempt to quantify the sensitivity of the Austrian forest ecosystems to acid deposition. Although first results have been obtained, further work is essential to improve the quality and reliability of model results and conclusions. Priority can be established for three subjects:

- Further analysis to improve data on base cation deposition. As has been indicated, base cation deposition can crucially influence the critical loads calculated with the developed model. At present, observations on base cation deposition are available only from a few monitoring stations and are limited to wet deposition only.

- Many of the important chemical relations established in the model could be verified by analysis of regional data sets for forest soils, which are available for Vorarlberg [8], Tirol [9] and Salzburg. Thereby, an increased understanding of the relevant soil processes can be obtained, enabling a more precise model formulation. In addition, these systematic data sets will also provide the necessary input data to operate the dynamic soil model, which enables also the simulation of possible recovery processes after a decline in acid deposition.

- The dynamic soil model can be considerably improved by extending it to several soil layers. Soil acidification would then be described for different layers within a soil profile and also take account of the different nutrient cycling processes. This means, that all rate-limited soil processes (root uptake, weathering, (de)nitrification) are described as a function of depth. The equilibrium processes (CO_2 equilibrium, carbonate and Al-hydroxide dissolution, cation exchange) do not change. Litterfall, mineralization and root uptake are considered to represent the most relevant nutrient cycling processes.

10   Conclusions

A model has been developed to simulate – with currently available data sets – dynamic acidification processes in forest soils as a function of acidic input from the atmosphere. The steady-state solution of this model has been used to determine the maximum long-term acid input into forest ecosystems that can be tolerated without damage to trees. These threshold values are termed as 'critical loads' and are currently determined for all of Europe to establish a general long-term goal for European environmental policies.

The analysis shows that acid deposition (resulting from SO_2, NO_x and ammonia emissions) is a potential danger for most of the Austrian forest ecosystems. Critical loads are the lowest

in the northern part of Austria (in the Wald- and Mühlviertel) and in the dry locations of the central alpine region.

Compared to acid deposition in 1985, critical loads have been exceeded in almost all parts of Austria. Particularly high exceedances (by more than a factor of five) have occurred in the eastern parts of Austria, in particular the oak forests in the Weinviertel, the Leithagebirge and the Wechsel region, where the transboundary contribution to acid deposition is high, and in the northern part of Austria (in the Wald- and Mühlviertel).

Further work is necessary to refine this first attempt to estimate environmental sensitivities of acid deposition in Austria. As the model shows, data improvements for base cation input and base saturation are most relevant to increase the accuracy of model results. Furthermore, an extension of this approach to take into account multi-layer processes including the nutrient cycles seems promising to simulate more precisely the tree damage resulting from soil acidification.

References

[1] Nilsson J. (1986) *Critical Loads for Nitrogen and Sulphur.* Nordisk Ministerrad, Miljo rapport 11.

[2] Iversen T., N. Halvorson, J. Saltbones and H. Sandnes (1990) *Calculated Budgets for Airborne Sulfur and Nitrogen in Europe.* EMEP/MSC-W Report **2/90**.

[3] Nilson S. and O. Sallnäs (1991) *Basic Data used by IIASA Forest Study for European Timber Assessment Analysis*, Forthcoming. Laxenburg, Austria: International Institute for Applied Systems Analysis.

[4] Sverdrup, H., W. deVries and A. Henriksen (1990) *Mapping Critical Loads: A Guidance Manual to Criteria, Calculations, Data Collection and Mapping.* Annex to chapter 4 of the Mapping Manual.

[5] deVries W. (1988) Critical Deposition Level for Nitrogen and Sulfur on Dutch Forest Ecosystems. *Water, Air, and Soil Pollution*, 42:221-239. Kluwer Academic Publishers.

[6] Hettelingh J.-P. and W. deVries (1990) *Mapping Vademecum*, Co-ordination Center West, RIVM, Bilthoven, The Netherlands.

[7] Kovar A. (1990) *in Press*, Technical University of Vienna, Austria.

[8] Husz G. (1986) *Lebensraum Vorarlberg, Grundlangenarbeiten zu Natur und Umwelt, Bodenzustandserhebung.* Vorarlberg, Austria.

[9] Stör D., H. Partl and M. Luxner (1989) *Bericht über den Zustand der Tiroler Böden 1988.* Amt der Tiroler Landesregierung. Innsbruck, Austria.

[10] Eliassen, A. and J. Saltbones (1983) Modeling of Long-Range Transport of Sulfur Over Europe: A Two-Year Model Run and Some Model Experiments. *Atmospheric Environment* 17:1457-1473.

[11] W. deVries, J. Kämäri and M. Posch (1989) Simulation of the Long-Term Soil Response to Acid Deposition in Various Buffer Ranges. *Water, Air, and Soil Pollution*, 48:349–390. Kluwer Academic Publishers.

[12] Alcamo J., R.S. Shaw and L. Hordijk (1990) *The Rains Model of Acidification. Science and Strategies in Europe.* Eds. Kluwer Academic Publishers.

[13] Reuss J.O., N. Christphersen and H.M. Seip (1986) A Critique of Model for Freshwater and Soil Acidification. *Water, Air, and Soil Pollution*, 30:909. Kluwer Academic Publishers.

[14] Johnson, A.H. (1982) *Assessing the Importance of Aluminum as a Link Between Acid Precipitation and Decreased Forest Growth*. Presented at USEPA Acid Deposition Effects Program, Raleigh, N.C., February.

[15] Huetterman, A. and B. Ulrich (1984) Solid Phase-solution root Interaction in Soils Subjected to Acid Deposition. London, United Kingdom: *Phil. Trans. R.* B 305:352-368.

[16] Fink, J. (1978) Karte der Böden und Standorteinheiten In: *6. Lieferung des Österrreich-Atlas*, Ed.: Österreichische Akademie der Wissenschaften, Wien.

[17] Baumgartner A., E. Reichel and G. Weber (1983) *Der Wasserhaushalt der Alpen*, Oldenbourg Verlag München Wien.

[18] Ivens W., A. Klein-Tank, P. Kauppi and J. Alcamo (1989) Atmospheric Deposition of Sulfur, Nitrogen and VAsic Cations onto European Forests: Observations and Model Calculations. In, *Regional Acidification Models. Geographical Extend and Time Development*. Edited by J. Kämäri. Springer Verlag.

[19] van Oene, H. (1991) *Acid Deposition and Forest Nutrient Imbalances: A Modeling Approach*. Accepted by Water, Air and Soil Pollution.